

## CHAPTER 3

# Data Analysis

*Chapter Leaders: E. Cook and K. Briffa*

*Chapter Contributors: S. Shiyatov, V. Mazepa, and P.D. Jones*

### 3.1. Introduction

*E. Cook and K. Briffa*

The information contained in annual tree rings is a valuable resource for studying environmental change. Past climate can be reconstructed from the year-to-year changes in annual ring width and ring density (e.g., Fritts, 1976; Schweingruber *et al.*, 1978). The occurrence of previously unrecorded geomorphological events, such as earthquakes and landslides, can be inferred from anomalous changes in the ring-width pattern (e.g., Shroder, 1980; Jacoby and Ulan, 1983). Forest-stand disturbances and gap-phase dynamics can be inferred from suppression-release patterns in tree rings (Brubaker, 1987), and, anomalous changes in the forest environment, due perhaps to anthropogenic pollutants, can be examined based on the recent patterns of tree rings (e.g., Eckstein *et al.*, 1983, 1984; Cook, 1987a). This list of applications is not complete. It is only intended to show that tree rings can be used to study a variety of environmental changes.

Although the use of tree rings for studying environmental change is widespread, the extraction of the desired signal from the unwanted noise can be difficult and uncertain. *Signal* is defined here, in a hypothesis-testing sense, as the information derived from tree rings that is relevant to the study of a particular problem. In contrast, *noise* is defined as the information that is irrelevant to the problem being studied. Given this reality, a tree-ring series is more appropriately thought of as the aggregation of several signals that become signal or noise only within the context of a specific hypothesis test or application. It is from this basis that the problem of signal extraction in tree-ring research is more fundamentally related to the disaggregation of the observed ring widths into a finite number of signals that represent the sum of the environmental influences on tree growth.

To provide a conceptual framework for this signal extraction problem, a linear aggregate model for tree-ring series will be described.

### 3.2. A Conceptual Linear Aggregate Model for Tree Rings

*E. Cook*

Consider a tree-ring series as a linear aggregate of several unobserved subseries. Let this aggregate series be expressed as

$$R_t = A_t + C_t + \delta D_{1t} + \delta D_{2t} + E_t ,$$

where:

- $R_t$  = the observed ring-width series;
- $A_t$  = the age-size-related trend in ring width;
- $C_t$  = the climatically related environmental signal;
- $D_{1t}$  = the disturbance pulse caused by a local endogenous disturbance;
- $D_{2t}$  = the disturbance pulse caused by a standwide exogenous disturbance; and
- $E_t$  = the largely unexplained year-to-year variability not related to the other signals.

This model is expressed in linear form to simplify the discussion of the concepts associated with each component of the model. It is known that certain ring-width properties are usually multiplicative (i.e., the relationship between the mean and standard deviation of ring widths). However, such nonlinear relationships can be easily linearized by transforming the ring widths to logarithms. In this sense, tree-ring series are intrinsically linear processes and the above formulation holds. The  $\delta$  associated with  $D_{1t}$  and  $D_{2t}$  is a binary indicator of the presence ( $\delta = 1$ ) or absence ( $\delta = 0$ ) of either class of disturbance at some time  $t$  in the ring widths. Thus,  $A_t$ ,  $C_t$ , and  $E_t$  are assumed to be continuously present in  $R_t$ , while  $D_{1t}$  and  $D_{2t}$  may or may not be present depending on whether the intervention of a disturbance has occurred at some time  $t$ . Some general properties of these subseries will now be described that are pertinent to the problem of estimating each one as a discrete process.

$A_t$  is a nonstationary process that reflects, in part, the geometrical constraint of adding a volume of wood to a stem of increasing radius. When this constraint is the principal source of the trend,  $A_t$  will exhibit an exponential decay as a function of time once the juvenile period of increasing radial increment has passed. This form of trend is most commonly found in trees growing in open environments where competition and disturbance effects are minimal. *Figure 3.1(a)* shows one such ring-width series from an open-canopy, semiarid site, ponderosa pine (*Pinus ponderosa*). More frequently, the behavior of  $A_t$  is strongly influenced and distorted by competition and disturbances in the forest.

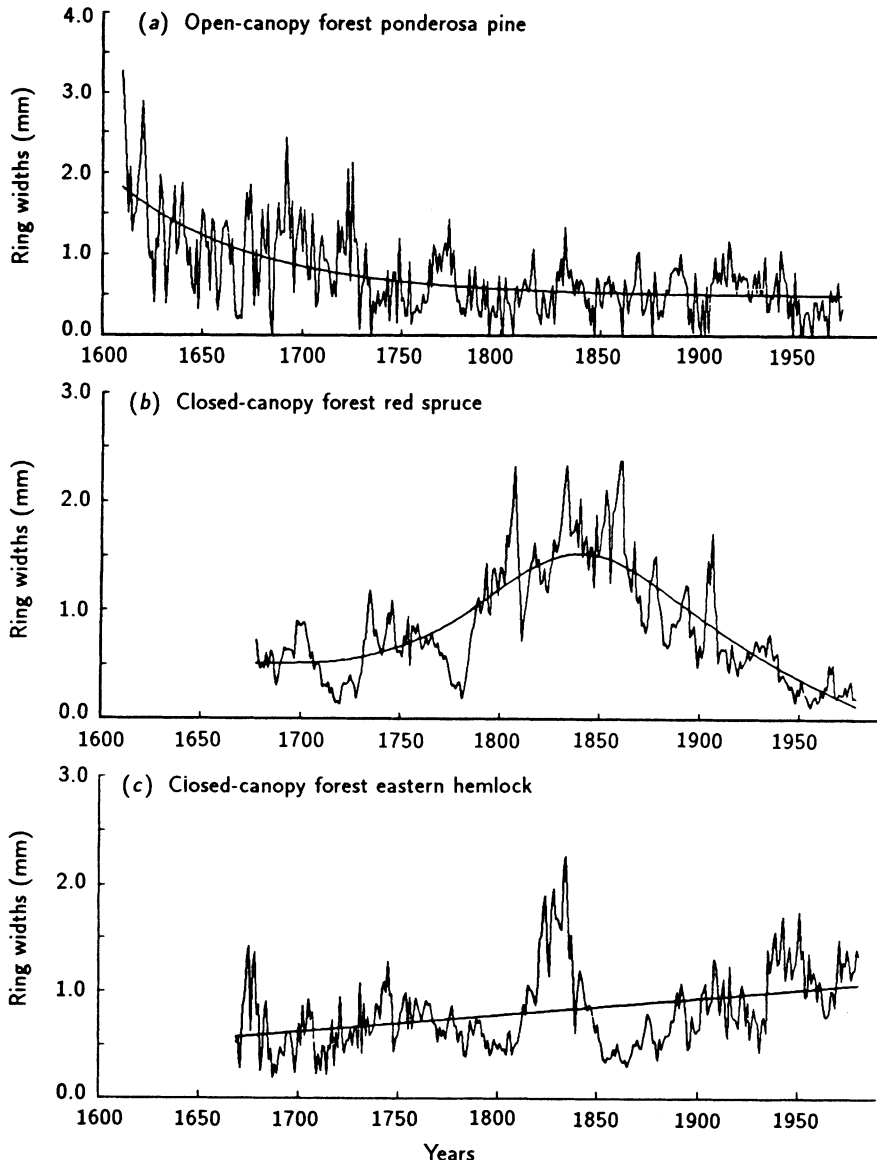


**Figure 9.1.** Three examples of the kinds of growth trends that can be found in ring-width data. Series (a) is from a semiarid site ponderosa pine (*Pinus ponderosa*), growing in an undisturbed, open-canopy environment. It shows the classic exponential decay of ring width that is expected when a tree ages, and when competition and disturbance are minimal. Figures (b) and (c) are from closed-canopy stands of red spruce (*Picea rubens*) and eastern hemlock (*Tsuga canadensis*). These latter two series show how the effects of competition and disturbance can radically alter the expected exponential decay of ring widths.

*Figures 3.1(b) and 3.1(c)* show two typical examples of this problem. The ring-width series in *Figures 3.1(b)* and *3.1(c)* are from a red spruce (*Picea rubens*) and an eastern hemlock (*Tsuga canadensis*), respectively. Each series shows the effects of suppression and release due to competition. These effects are common in stands of shade-tolerant species such as spruce and hemlock. It is clear from *Figure 3.1* that there is no predictable shape for  $A_t$  in the most general sense. That is,  $A_t$  does not necessarily arise from any family of deterministic growth curve models such as the negative exponential curve. Rather,  $A_t$  should be thought of as a nonstationary, stochastic process that may, as a special case, be modeled as a deterministic process (e.g., Fritts *et al.*, 1969).

$C_t$  represents the aggregate influence on tree growth of all climatically related environmental variables except for those associated with stand disturbances. Typical variables composing  $C_t$  are precipitation, temperature, and heat sums as they affect available soil-moisture supply, evapotranspiration demand, and phenology. These variables are assumed to be broad scale in that all the trees in a stand will be affected similarly by the same set of variables. Thus,  $C_t$  is a signal in common to all sampled trees in a stand. Some climatic variables that have been used to model  $C_t$  are monthly temperature and precipitation (Fritts, 1976), summer degree-days (Jacoby *et al.*, 1985), and drought indices (Cook and Jacoby, 1977). These variables can usually be regarded as stationary stochastic processes although they may be persistent in an autoregressive sense (Gilman *et al.*, 1963). Methods for modeling the composition of  $C_t$  in tree-ring chronologies, as response functions, are many and well researched (e.g., Fritts *et al.*, 1971; Meko, 1981; Guiot *et al.*, 1982b, Guiot, 1985a). A review of these methods is found in Chapter 5. Here,  $C_t$  will be regarded simply as the common climatic signal among all sampled trees without regard to its composition or properties.

The characteristic response of a tree to a local, or endogenous, disturbance in the forest is represented by  $D1_t$ . This response will be referred to as a pulse due to its expected transience and eventual disappearance in the ring widths. Endogenous disturbances are a consequence of gap-phase stand development in which individual trees are removed from the canopy by processes that do not affect the stand as a whole (White, 1979). This pattern of stand development creates patterns of suppression and release in the ring widths of trees adjacent to the trees removed from the canopy. See *Figure 3.1(b)* for a typical pattern of ring-width variation caused by gap-phase stand dynamics. Such natural competition effects are ubiquitous in closed-canopy forests. Forest management practices also fall within this class of disturbances when selective cutting, thinning, and the removal of undergrowth disturb only the local environment of trees in a stand.

An important property of endogenous disturbances, which is relevant to the disaggregation of  $R_t$ , is the likelihood that truly endogenous disturbances will be random events in both space and time within a forest stand of sufficient size. This means that the endogenous disturbance pulse in the ring widths of a given tree will be largely uncorrelated with endogenous disturbance pulses in other trees from the same stand. An example of this property is shown in *Figure 3.2*.

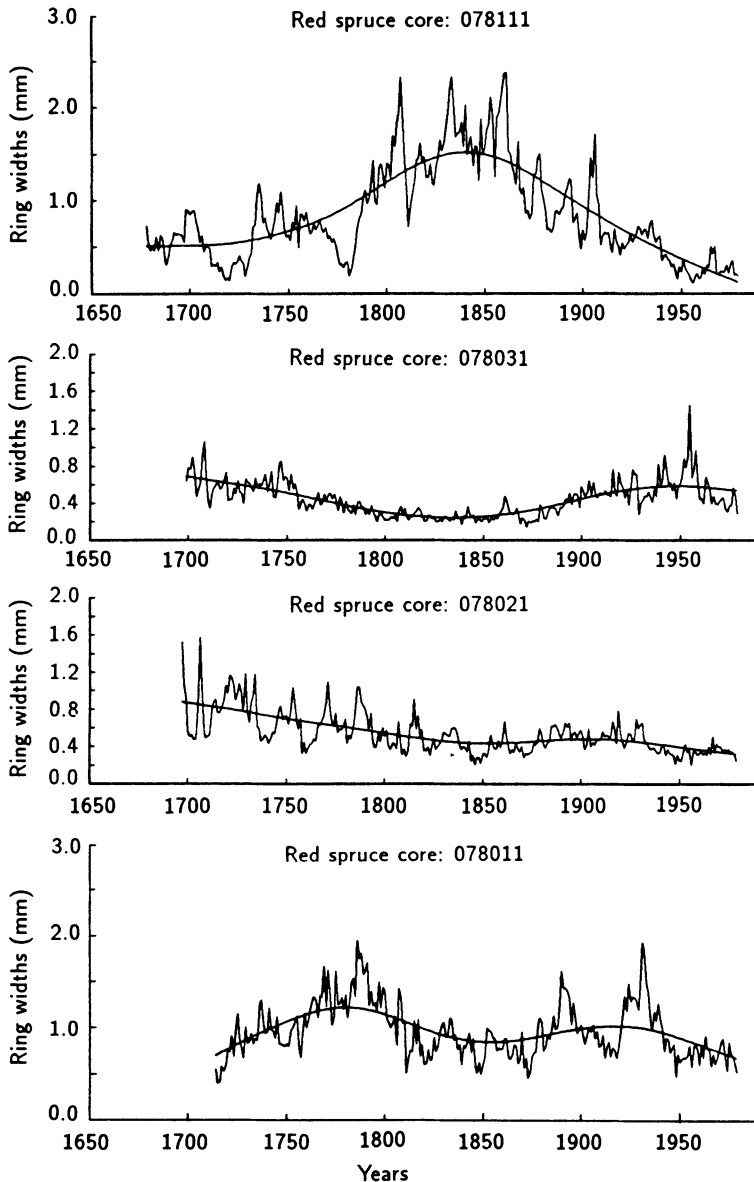


**Figure 9.2.** Four red spruce ring-width series from the same stand. Note the general lack of agreement in the long-term growth trends and also for shorter periods lasting 20–30 years. The lack of agreement is caused by differing competition and disturbance histories that alter the growth trends individually. These effects may be classified as endogenous disturbance effects due to the lack of synchrony among trees.

for four red spruce trees from the same stand. Each series has divergent or out-of-phase ring-width fluctuations lasting 20 or more years in length, which are likely to be due to endogenous disturbance events.

$D2_t$  represents the characteristic response of a tree to a standwide disturbance. Examples of non-climatic agents capable of producing a standwide disturbance are fire, insects, disease, logging, and perhaps pollution. Some episodic weather-related disturbance agents are severe frosts, high winds, and ice storms. The pertinent feature of the resultant exogenous disturbance pulse, which can differentiate it from that caused by an endogenous disturbance, is the synchrony in time of this event in all sampled trees from a stand. This indicates that  $D2_t$  will be a common feature among all trees, unlike  $D1_t$ . *Figure 9.3* shows some examples of an exogenous disturbance pulse in the ring widths of three eastern hemlock trees, which were all influenced by logging activity in the early 1900s. Note the sudden and synchronous increase in ring widths after about 1910 in all three series.

$E_t$  represents the unexplained variance in the ring widths after taking into account the contributions of  $A_t$ ,  $C_t$ ,  $D1_t$ , and  $D2_t$ . Some likely sources of  $E_t$  are, for example, microsite differences within the stand, gradients in soil characteristics and hydrology, and measurement error.  $E_t$  is assumed to be serially uncorrelated within and spatially uncorrelated between trees in the stand.

The conceptual model for ring widths based on the linear aggregate model indicates that a ring-width series may be broadly decomposed into a pure age trend component ( $A_t$ ), two common stochastic signal components ( $C_t$  and  $D2_t$ ), and two unique stochastic signal components ( $D1_t$  and  $E_t$ ). This breakdown into discrete classes assumes that there is no covariance between any of the components. That this assumption will not always hold is apparent when considering the problem of separating the trend component,  $A_t$ , from either disturbance pulse,  $D1_t$  and  $D2_t$ . If the response time of a tree to either kind of disturbance is short relative to the length of the ring-width series, then  $A_t$  may be differentiated from  $D1_t$  and  $D2_t$  within the limits of the method used to estimate  $A_t$ . However, if the ring-width series is short relative to the transient response to either kind of disturbance, than the trend component may, in fact, be largely composed of  $D1_t$ ,  $D2_t$ , or both.

In Section 3.3, methods of estimating and removing growth trends in ring-width data will be described, as part of the process of tree-ring standardization. Because of the potentially complicated character of these trends and the definition of what needs to be estimated as *trend*, the notation for the growth trend will be changed and generalized as follows. Let the estimated growth trend be defined as some deterministic or stochastic process

$$G_t = f(A_t, \delta D1_t, \delta D2_t) ,$$

where the estimated growth trend  $G_t$  is a function of the pure age trend component,  $A_t$ , and the stochastic perturbers of pure age trend,  $\delta D1_t$  and  $\delta D2_t$ . The  $\delta$  again means that these endogenous and exogenous disturbance effects need not be present in the observed ring-width series.

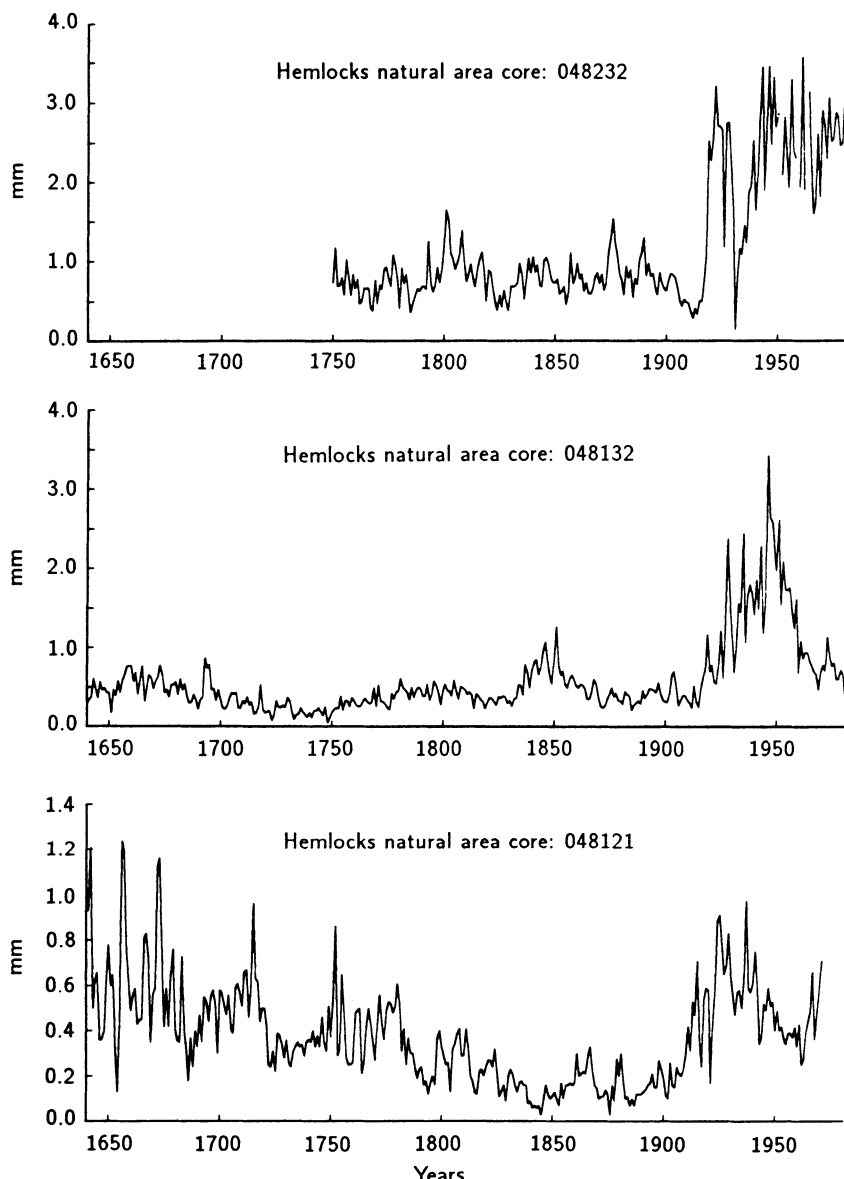


**Figure 9.9.** Three eastern hemlock ring-width series from a stand that has been affected by logging activity. It is known that the area around the hemlock stand was logged around 1910. Note the rapid increase in ring width in all three series at about that time. These synchronous changes in ring width due to a stand-level disturbance may be classified as exogenous disturbance effects.

This definition of  $G_t$  suggests that the common climatic component,  $C_t$ , may be the signal of interest, since  $A_t$ ,  $D1_t$ , and  $D2_t$  are considered collectively as non-climatic variance or noise. These definitions of signal and noise are implicit when standardizing tree-ring series for dendroclimatic studies (Fritts, 1976). They will be maintained throughout this section on tree-ring standardization and chronology development, with the realization that other applications of tree-ring analysis may define signal and noise differently.

### **3.3. Tree-Ring Standardization and Growth-Trend Estimation**

*E. Cook, K. Briffa, S. Shiyatov, and V. Mazepa*

#### **3.3.1. Introduction**

The estimation and removal of  $G_t$  from a ring-width series has been a traditional procedure in dendrochronology since its modern-day development by A.E. Douglass (1914, 1919). This procedure is known as standardization (Douglass, 1919; Fritts, 1976). Early workers searching for climatic signals in the ring-width series of old conifers identified long-term growth trends in measured ring-width data that could confidently be attributed solely to tree aging. In general, many factors can influence tree growth. However, by careful selection of long-lived trees growing in climatically stressed sites, early workers attempted to ensure that non-climatic growth influences such as competition and defoliation were minimized (Douglass, 1914). In this way, the selected trees were likely to have a strong climate signal, and the ring-width series were such that unwanted noise (resulting from tree aging) could be unambiguously identified. Schulman (1945b) described the purpose of standardization as follows:

To obtain a mean curve representing trees of various ages, the usual procedure is to "standardize" the individual tree curves by computing percentage departures from a trend line fitted to the curve and then to average the standardized values. Thus the large average growth rate of youth is reduced to conform with slower growth of maturity and old age.

From this quote, it is clear that the original intent of standardization was two-fold: (1) to remove non-climatic age trends from the ring-width series and (2) to allow the resultant standardized values of individual trees to be averaged together into a mean-value function by adjusting the series for differential growth rates due to differing tree ages and differences in the overall rate of growth. The "percentage departures" described by Schulman (1945b) are commonly known today as "tree-ring indices" (Fritts, 1976). Fritts and Swetnam (1986) provide an excellent description of the sequential process of trend removal, indexing, and averaging used in dendrochronology.

Standardization transforms the nonstationary ring widths into a new series of stationary, relative tree-ring indices that have a defined mean of 1.0 and a

relatively constant variance. This is accomplished by dividing each measured ring width by its expected value, as estimated by  $G_t$ . That is,

$$I_t = R_t / G_t \quad (3.1)$$

where  $I_t$  is the relative tree-ring index. When standardizing ring-width data, the indices are produced by division instead of differencing because ring-width series are heteroscedastic. That is, the local variance of ring widths is generally proportional to the local mean, where local is defined as some subinterval of time within the time span covered by the ring widths. The actual relationship is usually positive and linear between the ring-width means and their standard deviations when compared over time. *Figure 3.4(a)* shows a plot of 10-year mean ring widths versus their standard deviations for a collection of lodgepole pine (*Pinus contorta*) ring-width series. The positive correlation ( $r = .67$ ) is quite apparent. *Figure 3.4(b)* shows the same data after the ring-width series have been standardized using negative exponential and linear regression curves. The correlation between mean and standard deviation ( $r = .10$ ) is now largely gone.

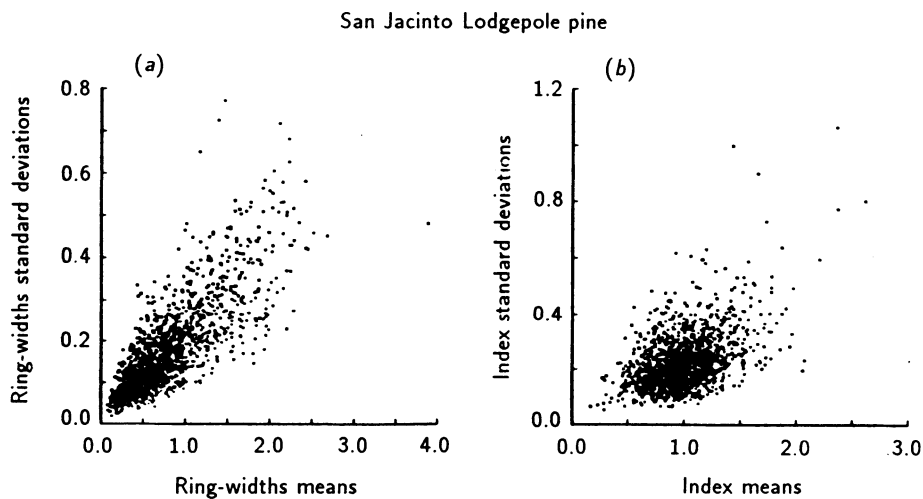


*Figure 3.4.* The relationship between the mean and standard deviation of tree-ring data before and after standardization. *Figure 3.4(a)* shows the scatter-plot of 10-year mean ring widths versus their standard deviations. The correlation is  $r = .67$ . In *Figure 3.4(b)*, after standardization and reduction of the ring widths to indices, the linear dependence between the mean and standard deviation is for the most part gone ( $r = .10$ ).

Another way of stabilizing the variance is by transforming the ring widths to logarithms. In this case, the resultant indices are computed by subtracting  $\log_e G_t$  from  $\log_e R_t$ , not by dividing as above. That is,

$$\log_e I_t = \log_e R_t - \log_e G_t \quad . \quad (3.2)$$

Problems arise in employing the logarithmic transformation to ring widths when the series has locally absent rings, which are typically coded as zero when using equation (3.1) to estimate  $I_t$ . Since the logarithm of zero does not exist, it has been suggested (e.g., Warren, 1980) that some arbitrarily small positive number replace the zero. This procedure may impart a statistically significant negative skew to the probability distribution of  $\log_e I_t$  if the chosen number is too small. In addition, a logarithmic transformation of the form in equation (3.2) may over-correct the heteroscedasticity and impart a negative dependence between the mean and standard deviation. Preliminary research indicates that the correct transformation of ring-width series to stabilize the variance is  $\log_e(R_t + c)$ , where  $c$  is a constant estimated from the series being transformed. That a simple logarithmic transformation will not be correct all of the time is illustrated in *Figure 3.5* for two white oak (*Quercus alba*) ring-width series. The lower series shows the typical linear dependence between the local 10-year means and their standard deviations [ $r = .77$ , *Figure 3.5(b)*]. A logarithmic transformation is clearly justified. In contrast, the upper ring-width series from the same stand of trees has no significant linear dependence between the local means and standard deviations [ $r = .08$ , *Figure 3.5(a)*]. Therefore, a logarithmic transformation is not justified in this case. These examples indicate the need for additional research to determine the best way to stabilize the variance of tree-ring indices by transformation.

The method of computing tree-ring indices as ratios has a long history in dendrochronology (Douglass, 1936; Schulman, 1956; Fritts, 1976). However, with the development of X-ray densitometry, additional tree-ring variables can be measured that also require some form of standardization. Bräker (1981) analyzed the properties of six tree-ring variables (total ring width, earlywood width, latewood width, latewood percentage, minimum earlywood density, and maximum latewood density) for conifer tree species growing in Switzerland. He found that latewood percentages and density data were properly standardized as differences from the estimated growth trend, not as ratios. Bräker (1981) justified the computation of differences because latewood percentages and density data do not usually show a clear dependence between mean and variance. However, Cleaveland (1983) found that maximum latewood densities of semiarid-site conifers in the western United States still required indexing by the ratio method to stabilize the variance. As more experience is gained in standardizing these comparatively new tree-ring variables, a preferred method of computing indices may be determined.

Because tree-ring indices are stationary processes having a defined mean and homogeneous variance, the index series of many trees from a site can be averaged together to form a mean-value function. Strictly speaking, it is not valid to average together nonstationary processes, like the majority of ring-width series, because such processes do not possess a defined mean or variance. While it is possible to compute the mean and variance of a ring-width series for a specific time period, it is incorrect to use these statistics as expectations for other

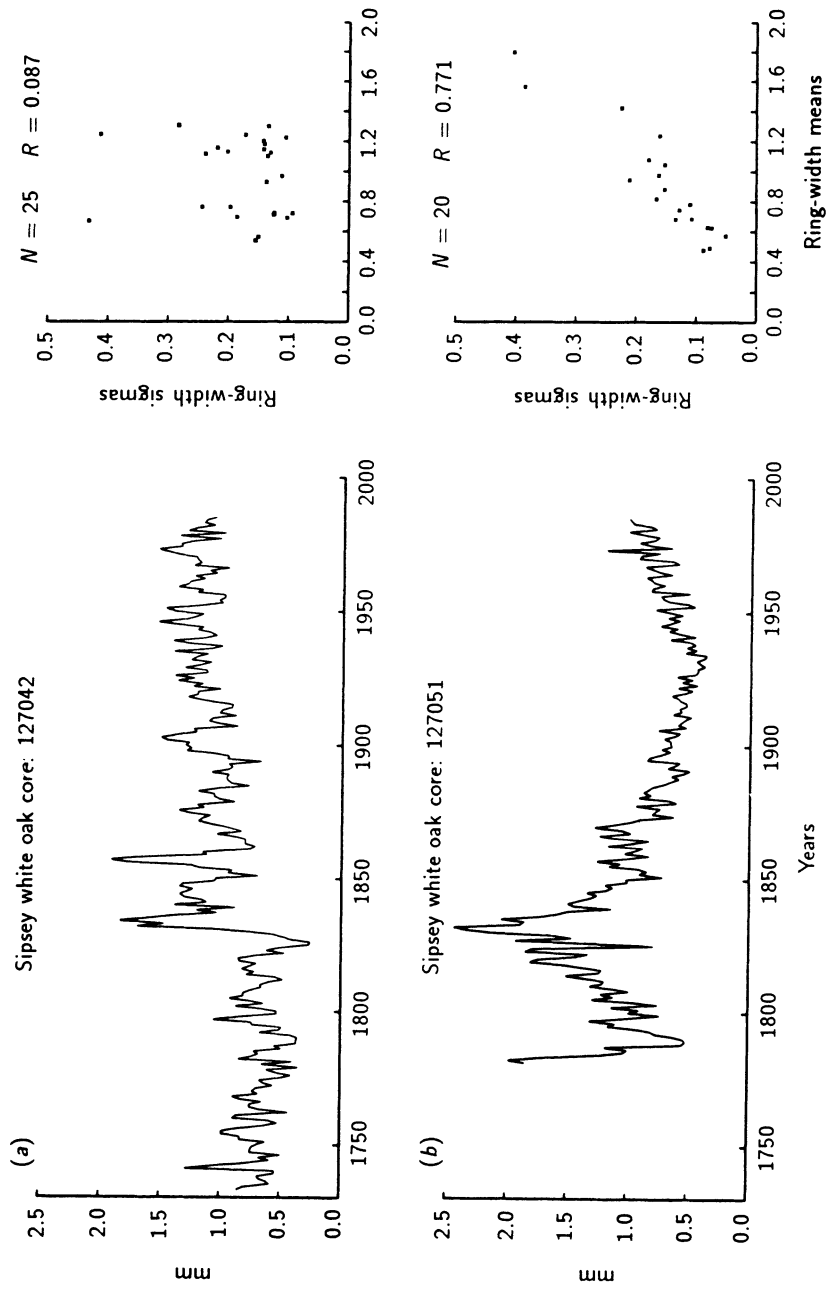


**Figure 9.5.** The variability in the mean-to-standard deviation relationship in two white oak (*Quercus alba*) ring-width series from the same stand. The bottom series (b) has the normally expected linear dependence, while the upper series (a) has no significant relationship. A logarithmic transformation to stabilize the variance would be appropriate for the lower series, but not for the upper series.

time periods or to use them as within-series estimates of the population parameters. This same problem carries through in a cross-sectional or between-series sense, where the lack of a defined sample mean makes the concept of estimating the between-series population mean invalid.

The mean-value function of tree-ring indices is frequently used to study past climate (Fritts, 1976). When climate (i.e.,  $C_t$  in the linear aggregate model) is the signal of interest, all other information in the ring widths (i.e.,  $A_t$ ,  $D1_t$ ,  $D2_t$ , and  $E_t$ ) is considered as noise and discarded as a compound form of  $G_t$  or minimized through averaging into the mean-value function.

Many methods are available for estimating  $G_t$ . They fall into two general classes: deterministic and stochastic. The deterministic methods typically involve fitting an *a priori* defined mathematical model of radial growth to the ring-width series, by the method of least squares. Ordinarily, it is assumed that  $G_t = f(A_t)$ , with  $D1_t$  and  $D2_t$  absent or negligible. The stochastic methods are more data-adaptive, and often are chosen by *a posteriori* selection criteria. These methods allow for the more general case,  $G_t = f(A_t, \delta D1_t, \delta D2_t)$ . As will be seen, each class of models has its advantages and disadvantages.

### 3.3.2. Deterministic methods of growth-trend estimation

The simplest deterministic model is the linear trend model, *viz.*,

$$G_t = b_0 + b_1 t , \quad (3.3)$$

where  $b_0$  is the y-intercept,  $b_1$  is the slope of the fitted linear regression line, and  $t$  is time in years from 1 to  $n$ . *Figure 3.1(c)* shows a linear trend line fit to a ring-width series. The slope coefficient,  $b_1$ , may be constrained to be negative or zero if the *a priori* expectation of  $G_t$  requires it. However, as noted earlier,  $G_t$  may also be negative exponential in form because of the *geometrical constraint* argument. Therefore, Fritts *et al.* (1969) suggest fitting the modified negative exponential curve of the form

$$G_t = a \exp^{-bt} + k , \quad (3.4)$$

where  $a$ ,  $b$ , and  $k$  are coefficients of this nonlinear regression function, all a function of time  $t$ . *Figure 3.1(a)* shows an example of this curve fit. Other functions have been used for estimating the age trend of ring-width series, such as the negative exponential curve (Fritts, 1963)

$$G_t = a \exp^{-bt} , \quad (3.5)$$

which is a special case ( $k = 0$ ) of equation (3.4); the hyperbolic function (Eklund, 1954)

$$1/G_t = a + b(t - k) , \quad (3.6)$$

where  $k$  is the middle year (i.e.,  $k = n/2$ ) of the series; the power function (Kuusela and Kilkki, 1963)

$$G_t = at^{-b} , \quad (3.7)$$

the generalized exponential or "Hugershoff" function (Warren, 1980; Bräker, 1981)

$$G_t = at^b \exp^{-gt} ; \quad (3.8)$$

and the Weibull probability density function (Yang *et al.*, 1978)

$$G_t = at^{a-1}b^{-a} \exp[-(t/b)^a] . \quad (3.9)$$

Equations (3.8) and (3.9) are able to fit both the juvenile increase in radial growth and the subsequent exponential decay of ring width as trees mature. These functions are more theoretically complete than the other models, which can only fit the maturation phase of declining radial growth.

These deterministic models produce monotonic or unimodal curves, which clearly require that the observed growth trend be simple in form. However, Warren (1980) made his fitting procedure much more general by allowing the age trend to be modeled as a temporal aggregate of generalized exponential functions. This allowed Warren (1980) to fit a series of suppression-release events in his tree rings. And, except for equations (3.3) and (3.4), all have a limiting value of zero for  $G_t$  as  $t$  grows large. This property is unsatisfactory for many trees that approach a constant level of ring width in old age, hence the preference for equation (3.4) over equation (3.5) by Fritts *et al.*, (1969) for standardizing semiarid-site, old-age conifers. The deterministic growth-trend models described above are most appropriate for open-canopy stands of undisturbed trees and for young trees with strong juvenile age trends. It is also clear that these models only depend on time  $t$  for predictive purposes. Thus, they are deterministic. The last two models [equations (3.8) and (3.9)] have not been widely used in dendrochronology, although their use in forest mensuration to estimate growth increment functions is more common.

Another family of deterministic growth-trend models is found in polynomial detrending (Jonsson and Matern, 1974; Fritts, 1976; Graybill, 1979). This model for  $G_t$  has the form

$$G_t = b_0 + b_1 t + b_2 t^2 + \cdots + b_p t^p . \quad (3.10)$$

The linear-trend model is just a special case of this polynomial model. This method of growth-trend estimation is not based on any *a priori* age-trend model. Rather, a best-fit, order- $p$  polynomial, which is initially unknown, is fit to a ring-width series based on the behavior of that series alone. It is far more *ad hoc* and data adaptive than the previous models, although it still maintains its dependence on time alone for predictive purposes. Polynomial detrending of the form above suffers from problems of order selection, potentially severe end-fitting problems, and poor local goodness-of-fit (Cook and Peters, 1981; Briffa, 1984; Cook, 1985). In spite of their wide usage in the past, polynomials of the form of equation (3.10) are not recommended as a general method for detrending ring-width series.

In the rare situations where the age trend is known to have a simple deterministic form based on theoretical considerations, the best approach is to describe that trend with an appropriate mathematical model. This is the most concise and directly communicable way of describing and explaining the character of the age trend. Nevertheless, assuming a mathematical function for describing trends in tree growth may be unnecessarily restrictive. Problems increasingly arise when this approach is used in situations where trends are complex or where it is necessary to remove relatively medium or short time scale variation in tree-ring data during standardization. Functional growth equations are often too simple.

A more basic weakness of the method is that the goodness-of-fit varies with time because of time-dependent stochastic departures from the theoretical model. Thus, noise-related medium-frequency variance may be retained in some parts of the series, yet removed in others. This may introduce spurious medium frequency variations into the standardized series.

Given the inherent limitations and potential problems of deterministic growth-trend models in fitting the low- and middle-frequency stochastic perturbations commonly found in ring-width series (see *Figures 3.1–3.3*), stochastic methods of growth-trend estimation have been investigated. These methods fall within the realms of low-pass digital filtering (Parker, 1971; Cook and Peters, 1981; Briffa *et al.*, 1983), exponential smoothing (Barefoot *et al.*, 1974), and differencing (Box and Jenkins, 1970). These methods will be described next.

### 3.3.3. Stochastic methods of growth-trend estimation

#### *Low-Pass Digital Filtering*

Low-pass digital filtering typically involves passing an odd-numbered set of symmetrical, low-pass filter weights over a ring-width series to produce a smoothed estimate of the actual series. This is accomplished as

$$G_t = \sum_{i=-n}^{+n} w_i R_{t+i} / \sum_{i=-n}^{+n} w_i , \quad (3.11)$$

where  $G_t$  is the  $t$ th filtered value and where  $w_i$  is the weight by which the value of the series  $i$  units removed from  $t$  is multiplied. There are  $2n+1$  filter weights. Equation (3.11) clearly shows that this digital filter is a centrally weighted moving average of the actual data. The  $w_i$  tapers off equally on both sides of the maximum central weight until the outermost weights are arbitrarily close to zero. These weights may be derived from the Gaussian probability distribution function and tailored to have a particular frequency response (Mitchell *et al.*, 1966; Briffa, 1984). Alternately, the cubic-smoothing spline can be used as a symmetrical, low-pass digital filter (Cook and Peters, 1981), without the need to compute explicitly the filter weights.

Symmetrical filters of this type preserve the original phase information of the unfiltered time series in the filtered values. In the past, equally weighted (i.e.,  $w_i = 1.0$  for all  $i$ ) moving averages have been advocated for standardizing tree-ring series (e.g., Bitvinskas, 1974). This form of digital filter cannot be recommended under any circumstances because it causes undesirable phase shifts in the smoothed age-trend estimates and distortion in the power spectrum of the resultant standardized tree-ring indices. Fritts (1976) and Briffa (1984) detail the use of digital filters in tree-ring analysis.

The degree of smoothness of the low-pass filter estimates of  $G_t$  depends on the characteristic frequency response of the filter. For the Gaussian filter, the response is approximately

$$u(f) = \exp(-2\pi^2 s_G f^2) , \quad (3.12)$$

where  $s_G$  equals  $L/6$  and  $L$  is the length of the filter (Briffa, 1984). For the cubic-smoothing spline (Cook and Peters, 1981), the frequency-response function is computed as

$$u(f) = 1 - \frac{1}{1 + \frac{p(\cos 2\pi f + 2)}{6(\cos 2\pi f - 1)^2}} , \quad (3.13)$$

where  $p$  is the Lagrange multiplier that uniquely defines the frequency response of the spline. The 50% frequency-response cutoff, which is the frequency at which 50% of the amplitude of a signal is retained (or removed), is typically used to define the degree of smoothing by a digital filter. For the smoothing spline, it can be defined in terms of  $p$  as

$$p = \frac{6(\cos 2\pi f - 1)^2}{\cos 2\pi f + 2} . \quad (3.14)$$

Equations (3.12)–(3.14) assume a sampling interval of one year, which is typical for tree-ring series. *Figure 9.6* shows some characteristic frequency-response functions of the Gaussian filter and smoothing spline. The transition bandwidth

of each filter, which is defined as the bandwidth of frequencies between  $u(f) = 0$  and  $u(f) = 1$ , is rather broad in each case. The response of the spline filter is steeper than that of the Gaussian filter, which means that the latter will leave in slightly more low-frequency variance for a given 50% response cutoff. Although the transition bandwidths in *Figure 9.6* could be criticized for being too broad, they are probably satisfactory for estimating  $G_t$  – given the considerable uncertainty in knowing what degree of smoothing to use.

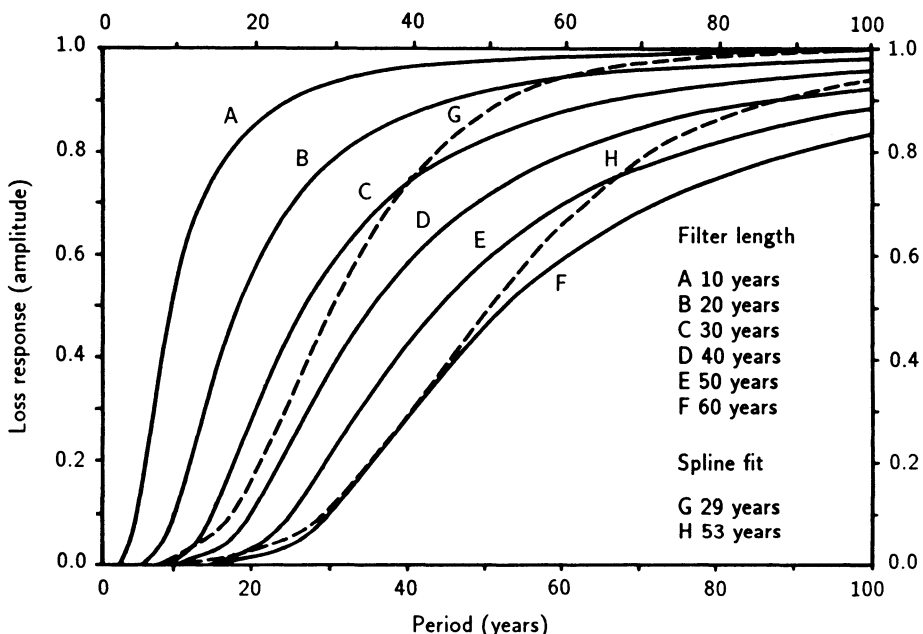


**Figure 9.6.** Some characteristic frequency-response functions of the Gaussian filter (solid curves) and the cubic-smoothing spline (dashed curves). The 50% frequency-response cutoff in years is given for each filter. (Modified from Briffa, 1984.)

There is often little theoretical basis for selecting the *proper* degree of curve flexibility or data smoothing when using digital filters. For this reason, a chosen digital filter can be rather difficult to justify. Briffa *et al.* (1983) used *a priori* information about stand-management practices in Europe to select the frequency response for their low-pass filter used in estimating  $G_t$ . Their selection criterion is based on the concept that the unwanted noise in the ring widths is frequency dependent (Briffa *et al.*, 1986). In this case, it was felt that the noise was largely restricted to wavelengths longer than about 50 years. A similar determination was made by Cook and Peters (1981) and Blasing *et al.* (1983), based on using the cubic-smoothing spline as a digital filter on ring widths from North American trees. However, the filters advocated by these studies may be too flexible for general use.

Given that the frequency dependent properties of the noise (i.e., the band-limited spectral properties of the age trend and stochastic disturbance effects) will be unknown *a priori* in many situations, how might the *appropriate* or *optimal* frequency response be selected objectively? One possible criterion is based on the signal-to-noise ratio (SNR) (Wigley *et al.*, 1984). The SNR is defined as

$$\text{SNR} = N \bar{r} / (1 - \bar{r}) , \quad (3.15)$$

where  $\bar{r}$  is the average correlation between trees and  $N$  is the number of trees in the ensemble of standardized tree-ring indices. SNR is an expression of the strength of the observed common signal among trees in the ensemble. Tuning the frequency response of the digital filter to maximize the SNR would seem to be one optimal and objective criterion. Two examples, in *Table 3.1*, show how the SNR of tree-ring indices can change as the frequency response of a Gaussian filter is tuned to maximize that criterion. In example A, a peak in SNR is indicated for the filter with a 50% frequency response of 40 years. However, for example B, the SNR increases all the way to the minimum 50% frequency response of 10 years. This result indicates that there may not be a clear maximum SNR in the low-to-intermediate frequencies of some tree-ring chronologies, which will make the application of the maximum SNR criterion more difficult. The maximum SNR criterion is also flawed because it assumes, in the derivation of equation (3.15), that the series being cross-correlated is serially random. This means that the SNR is best suited for measuring the strength of the observed high-frequency signal in the tree-ring indices, not the persistent, low-frequency signal that may of interest in the study of climatic change. Thus, the maximum SNR criterion may be biased toward selecting a digital filter that removes an excessive amount of low-frequency variance during standardization.

*Table 3.1.* The effect of different Gaussian low-pass filters on the fractional common variance ( $\bar{r}$ ) and signal-to-noise ratio (SNR) of an ensemble of standardized tree-ring indices (Briffa, 1984). The tree-ring data are from oak sites in the United Kingdom. The 50% frequency response of each filter is given in years. Each analysis is based on 14 trees for the time period 1880–1979.

<i>Example A</i>			<i>Example B</i>		
<i>Filter length</i>	$\bar{r} \times 100$	<i>SNR</i>	<i>Filter length</i>	$\bar{r} \times 100$	<i>SNR</i>
10 years	30.09	6.03	10 years	46.54	20.03 <sup>a</sup>
20 years	30.90	6.26	20 years	41.93	16.61
30 years	32.08	6.61	30 years	39.18	14.81
40 years	32.83	6.84 <sup>a</sup>	40 years	38.06	14.14
50 years	32.77	6.83	50 years	37.53	13.82
60 years	32.42	6.72	60 years	36.94	13.47

<sup>a</sup>Denotes the maximum  $\bar{r}$  and SNR.

Blasing *et al.* (1983) examined another objective criterion for choosing the optimum filter response of the smoothing spline. They selected a filter for standardization that produced the best tree-ring chronology for dendroclimatic reconstruction. In their example, Blasing *et al.* (1983) reconstructed total annual precipitation for Iowa from white oak (*Quercus alba*) tree-ring chronologies standardized with splines of differing frequency response. They determined the optimum frequency response from the chronology, which produced the reconstruction that verified best against independent data. In this case, the optimum spline had a 50% frequency response of about 50 years, a value similar to example A in *Table 3.1*. It is not clear whether this technique will be widely applicable, however, because it depends on having long, homogeneous climatic records for reconstruction and verification. This will not be the case for many regions of the world where tree-ring analysis can be done. In addition, this optimization rule depends on having tree-ring data that can strongly model the climatic data. This may not be the case in many mesic forest environments where climate has a weaker and less-direct impact on tree growth than was the case for the Iowa oaks.

Another possible criterion for objectively selecting an optimal digital filter for standardization is related to the concept of "trend in mean" (Granger, 1966). From the theory of spectral analysis (Jenkins and Watts, 1968), the lowest-frequency harmonic that can be theoretically resolved in a time series has a frequency  $f = 1/n$ , where  $n$  is the length of the series. This is the fundamental frequency of the process (Jenkins and Watts, 1968). The fundamental frequency corresponds to one complete sine wave with a cycle length of  $n$  years. According to the definition of trend in mean, any variance at wavelengths longer than the observed time series ( $f < 1/n$ ) cannot be differentiated from pure trend ( $f = 0.0$ ), unless strong *a priori* information on climatic variability and the properties of the ring-width data allow for it. For example, if it is known that the sampled trees are temperature sensitive and that the trend in temperature for the recent past has been positive for the region where the trees were sampled, then any positive trend in ring width may be related to the positive trend in temperature. In this case, ring-width series with positive trends should be standardized with deterministic curves that are constrained to be non-positive in trend. Obviously, care must be taken to ensure that the observed positive trend in ring width is not due to non-climatic effects, such as a release from competition. However, for the majority of cases, trend in mean can be used as the basic definition of the theoretical resolvable limit of climatic information in tree-ring chronologies.

Given the above definition of trend in mean, another objective criterion for selecting the optimal frequency response of a digital filter is as follows. Select a 50% frequency-response cutoff in years for the filter that equals some large percentage of the series length,  $n$ . This is the  $\%n$  criterion described in Cook (1985). The results of Cook (1985) suggest that the percentage is 67% $n$  to 75% $n$  based on using the cubic-smoothing spline as a digital filter. The  $\%n$  criterion ensures that little low-frequency variance, which is resolvable in the standardized tree rings, will be lost in estimating and removing the growth trend. This criterion also has a bias of sorts because of the stiff character of the low-pass filter estimates of the growth trend. It will not necessarily guarantee and, in fact, will

rarely possess any kind of optimal goodness-of-fit. Thus, the SNR of an ensemble of tree-ring indices standardized by the  $\%n$  criterion will usually be inferior to those standardized by the maximum SNR criterion. The SNR of  $\%n$  standardized indices can, of course, be increased by adding additional trees to the ensemble. Additional increases in SNR are also possible by prewhitening the detrended indices as autoregressive processes and by using a robust mean in estimating the mean-value function (Cook, 1985). The last two approaches will be described in Sections 3.4.2 and 3.4.3. Either way, the drawback of lower SNR for the  $\%n$  method can be ameliorated.

Figure 3.7 compares cubic-smoothing spline estimates of  $G_t$  for three red spruce ring-width series using a 67% $n$  criterion (solid line) and a fixed, 50% frequency-response cutoff of 60 years (dashed line). The 60-year cutoff is not the exact maximum SNR criterion, but it is much closer to it than the 67% $n$  curves. The differences in the curve fits are readily apparent. The 67% $n$  criterion does a poor job in tracking medium-frequency (10–30 years) fluctuations within each series that sometimes disagree with contemporaneous fluctuations in the other series. Examples of this lack of synchrony are found in the 1850s and 1950s of series (b). If signal is defined as information in the tree rings that is common to all trees in the ensemble, then the 67% $n$  criterion does not eliminate noise as well as the 60-year cutoff. On the basis of noise reduction performance alone, the adequacy of the 67% $n$  criterion will usually depend more on sufficient replication to average out endogenous-style growth fluctuations and on additional noise reduction techniques such as robust mean estimation and autoregressive modeling. All of these noise reduction techniques assume that common, exogenous non-climatic variance ( $D2_t$ ) is not present in the ensemble. If  $D2_t$  variance is known to be present either *a priori* or by strong inference, then more flexible filters may be necessary to remove that component.

The  $\%n$  and maximum SNR criteria represent two reasonable and objective limits for selecting the frequency response of the digital filter and, therefore, the degree of flexibility of the resultant low-pass filter estimates of the age trend. If high-frequency information is of sole interest in a tree-ring chronology, then the latter criterion will probably be preferred if other noise reduction techniques, such as autoregressive modeling, are not used. However, if tree-ring series are to be used to study climatic and environmental change at virtually all resolvable wavelengths in a tree-ring chronology, then the  $\%n$  criterion should be considered as a criterion of smoothness for the digital filter.

Although digital filtering, as described above, is attractive for estimating the non-climatic growth trend in ring-width series, a theoretical drawback of this method should be noted. The symmetry of the filter weights in equation (3.11) requires both past and future ring widths to estimate the central smoothed value for each year. This model for low-frequency changes in ring width is obviously incorrect because trees cannot possibly anticipate radial growth performance of future years in developing an expectation for ring width for the current year. The predisposition to grow at a certain potential rate must come only from the past. This means that one-sided or causal filters (Robinson and Treital, 1980) of the general form

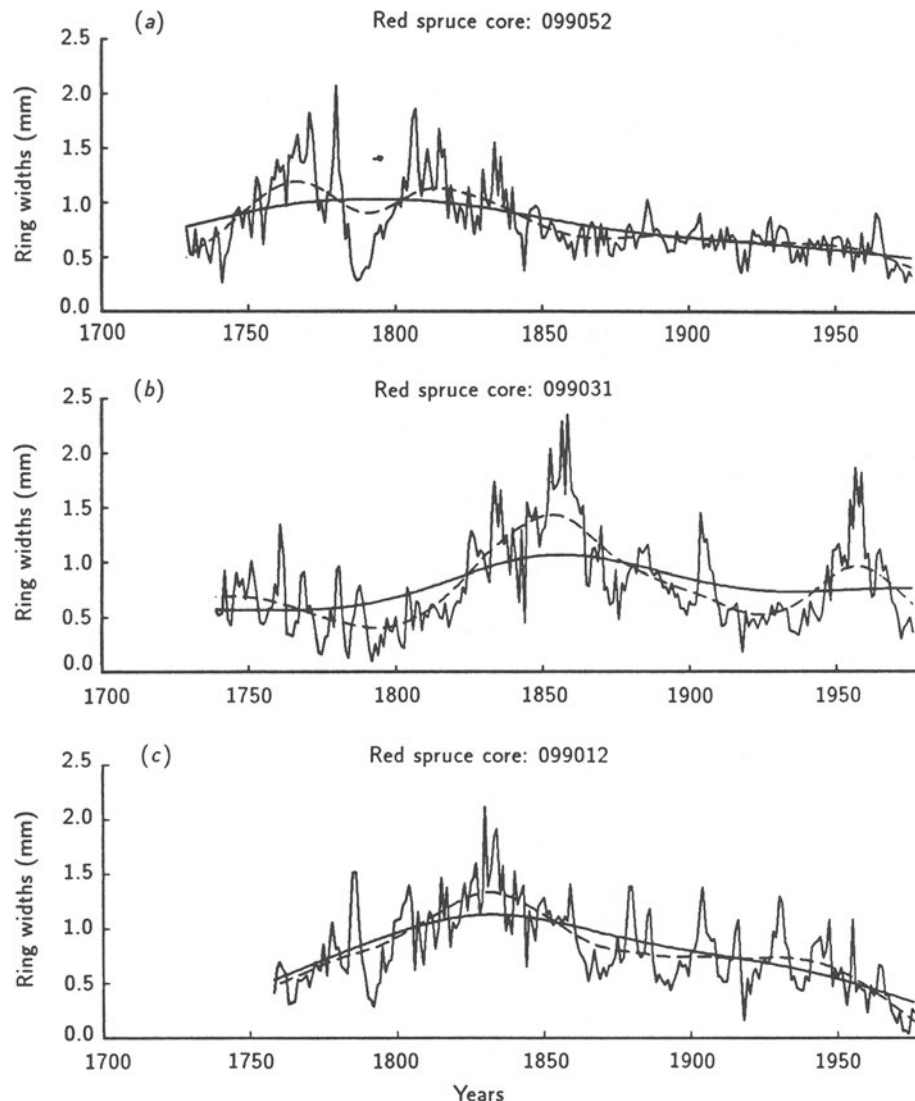


**Figure 3.7.** A comparison of two selections of smoothing ring-width data using the cubic-smoothing spline. The solid lines indicate spline values based on a 50% frequency-response cutoff of  $67\%n$ , where  $n$  is the series length in years. The dashed lines indicate splines with fixed 50% frequency-response cutoffs of 60 years. The more flexible curve fit is clearly superior on an individual series basis. However, with sufficient replication and the use of other noise reduction techniques, the  $\%n$  criterion may be used if the need to preserve potentially resolvable long-term climatic variance is important.

$$Z_t = \sum_{i=1}^{-\infty} \Psi_i e_{t-i} + e_t \quad (3.16)$$

are more appropriate for modeling certain aspects of the persistence or predictability in ring width from year to year. Equation (3.16) is the general linear process, which serves as the foundation for autoregressive-moving average (ARMA) time series modeling (Box and Jenkins, 1970). The general linear process and its finite ARMA derivatives are causal filters because only current and past information is necessary for the evolution of the observed process. The use of ARMA models in tree-ring chronology development will be described more fully, later.

### *Exponential Smoothing*

A quite different stochastic estimate of  $G_t$  is possible by using exponential smoothing (Barefoot *et al.*, 1974). The smoothing function chosen by Barefoot *et al.* (1974) consists of two components: an average,  $\bar{R}_t$ , and a lag correction for trend,  $\tilde{R}_t$ . This is expressed as

$$G_t = \alpha \bar{R}_t + (1 - \alpha) \alpha \tilde{R}_t , \quad (3.17a)$$

where  $G_t$  is the smoothed estimate for year  $t$ ,

$$\bar{R}_t = \alpha (R_t - 1) + (1 - \alpha) (\bar{R}_{t-1}) , \quad (3.17b)$$

and

$$\tilde{R}_t = \alpha (R_t - R_{t-1}) + [(1 - \alpha)/\alpha] (\tilde{R}_{t-1}) . \quad (3.17c)$$

The quantity  $\alpha$  is a weighting factor that determines the degree of smoothing or how much past information on ring width enters into the current estimate. The influence of past ring widths decays exponentially as  $(1 - \alpha)^n$ , where  $n$  is the number of years prior to the current estimate. Barefoot *et al.* (1974) selected  $\alpha = 0.2$  to smooth their ring widths, which allows the previous 10–15 years of data to influence the current estimate of  $G_t$ . In contrast to the symmetrical digital filter, exponential smoothing operates as a one-sided, causal filter (Robinson and Treitäl, 1980) that only relies on current and prior values in its estimation. As noted earlier, this is a desirable property in that the estimates of  $G_t$  evolve through time in the same way that trees grow. However, the selection of  $\alpha$  may be series dependent and difficult to select. In this sense, it has the same problem as digital filtering.

Abraham and Ledolter (1983) review exponential smoothing techniques and suggest selecting an  $\alpha$  that minimizes the one-step ahead prediction error variance. This criterion for  $\alpha$ , if adequate, will produce a series of random residuals from the smoothing function. Except in rare cases where a serially random tree-ring series is of interest, an  $\alpha$  based on minimizing the prediction mean-square error will remove too much low-frequency variance for climatic studies. The one-sided form of equation (3.17a) is conceptually appealing, but additional research is needed on developing objective guidelines for choosing the smoothing constant for tree-ring standardization.

### *Differencing*

Another method of stochastic detrending is based on differencing (Box and Jenkins, 1970; Van Deusen, 1987). In this approach, a ring-width series is considered to be a random walk with deterministic drift. This process has the form

$$R_t = R_{t-1} + e_t + \delta , \quad (3.18)$$

where  $R_t$  is the observed ring width,  $e_t$  is a serially uncorrelated random shock, and  $\delta$  is the deterministic drift of the process that may also be thought of as a constant slope parameter. By taking first differences of  $R_t$  (usually after logarithmic transformation) as

$$\nabla R_t = R_t - R_{t-1} , \quad (3.19)$$

the deterministic drift, which imparts linear trend to the  $R_t$ , is nothing more than the arithmetic mean of  $\nabla R_t$ . However, the trend that is removed by differencing is actually stochastic, rather than deterministic. This is easily seen by noting that the conditional expectation of  $R_t$  given  $R_{t-1}, R_{t-2}, \dots$  is  $E(R_t) = R_{t-1} + \delta$ . Since  $R_{t-1}$  is subject to random shocks in the form of  $e_t$ , the deterministic trend component of  $E(R_t)$  is also subjected to random shocks. Thus, the trend changes stochastically.

The advantage of differencing lies in its simplicity, causal structure, and total objectivity. There are no parameters to estimate, and the method is insensitive to ring widths more than one year apart. The latter property makes differencing especially attractive when old tree-ring collections are updated. The addition of new rings to each series will have no effect on the way that the detrended tree rings are produced. In this sense, differencing is locally robust as a detrending method when new data are added, which is not the case for deterministic least squares methods of detrending.

The disadvantage of differencing is the way in which the method acts as a high-pass filter. Virtually all low-frequency variance is attenuated and the high, year-to-year variance is emphasized. This property follows from the notion that the differenced series is nothing more than a numerical estimate of the 1st-

derivative of the process (Van Deusen, 1987). Thus, each differenced value is the relative rate of change in ring width from one year to the next. The severe attenuation of low-frequency variance in the first differences means that the resultant tree-ring chronology will not exhibit the year-to-year persistence commonly seen both in climate (Gilman *et al.*, 1963; Mitchell *et al.*, 1966) and in tree rings standardized by other detrending methods (Rose, 1983; Monserud, 1986). This deficiency can be ameliorated through the use of ARMA time series modeling techniques, which are described in the next section.

Differencing has only recently been applied to the problem of tree-ring detrending and standardization (Van Deusen, 1987; Guiot, 1987a). Because of this and its importance in autoregressive-integrated moving average (ARIMA) time series modeling (Box and Jenkins, 1970), it deserves additional research and testing.

### 3.3.4. Other methods of estimating growth trends

Other techniques can be used for estimating growth trends that do not clearly fit into the simple categories of techniques just described.

*Graphic techniques.* In the precomputer era of dendrochronology, growth trends were frequently estimated visually using flexible rulers (Schulman, 1956; Stokes and Smiley, 1968). Although this method has an inherently subjective aspect to it, it can be applied with a high degree of uniformity by experienced individuals when the growth trend is simple in form (i.e., negative exponential and linear). However, with the availability of digital computers and programs for estimating satisfactory growth trends, this method is rarely applied today.

*Stand-level growth trends based on the biological age of trees.* Another method of growth-trend estimation has been described by Erlandsson (1936), Mitchell (1967), and Komin (1987). It is based on collecting ring-width material from a large range of age classes of a given tree species. The ring-width measurements of each sample are aligned with those of the other samples according to the biological age of the rings, not the chronological age. For example, year five of a 200-year-old tree is aligned with year five of a 50-year-old tree by this method. Once the biological age alignment is done, the ring widths of all samples are averaged together to produce a tree-based, average biological growth trend. The averaging process greatly attenuates the yearly fluctuations in ring width due to environmental factors because of the chronological misalignment of the tree rings. Consequently, the underlying growth curve is emphasized. The degree to which the environmental effects are attenuated will depend on the sample size for each year, the distribution of tree ages in the collection, and the level of randomness through time of the environmental factors. The estimation of the mean growth curve also assumes that the structural form of the curve at any biological age is independent of the time period during which it is produced. There seems to be little room for endogenous and exogenous disturbance effects in this model.

Once the mean growth curve is estimated, a smooth mathematical function is fit to the curve and used to standardize the individual series from the site (Mitchell, 1967; Komin, 1987). Fritts (1976, page 280) points out that this method is flawed as a technique of tree-ring standardization. He notes:

All individuals of a species rarely attain optimum growth at the same age, and individual trees differ in their growth rates because of differences in soil factors, competition, microclimate, and other factors governing the productivity of the site. Therefore, individual trees will deviate markedly and systematically from the mean growth curve.

These reasons are sufficient to reject the method as a standardizing tool for dendroclimatic studies. However, where the signal of interest is the variance within each series that deviates from the mean growth curve of the stand, this method is appropriate.

*The corridor method.* Shiyatov (1987) describes another approach to standardization called the corridor method. It is based on the construction of a maximum possible growth curve and a minimum possible growth curve for each ring-width series. These two curves form a growth corridor within which the range in ring-width variability fluctuates. Figures 3.8(a), 3.8(c), and 3.8(e) illustrate some common forms of the corridor, which is usually constrained to evolve smoothly through time. The maximum growth curve is based on a few ring widths that define the local maxima in the ring-width series. Typically, it displays the most pronounced growth trend and is usually constrained to have only one peak (Shiyatov and Mazepa, 1987). The minimum growth curve is based on a few ring widths that define the local minima in the series. It tends to have a less pronounced growth trend and may be constrained to repeat the bends of the maximum curve (Shiyatov and Mazepa, 1987). Where the ring widths get very small or when there is a high frequency of locally absent rings, the minimum curve approaches or equals zero [e.g., Figures 3.8 (a) and 3.8(e)].

The tree-ring indices are calculated from the corridor estimates as

$$I_t = \frac{R_t - G1_t}{G2_t - G1_t} * 100 \quad (200) , \quad (3.20)$$

where  $I_t$  is the index,  $R_t$  is the ring width,  $G1_t$  is the minimum growth-curve estimate, and  $G2_t$  is the maximum growth-curve estimate, all for year  $t$ . The 100 (200) are scaling factors that transform the index into either percentages (\* 100) of the corridor width or  $2 \times$  percentages (\* 200).

A comparison of equation (3.20) with the more commonly used formula for computing indices, equation (3.1) reveals the difference in the techniques. The indices computed from equation (3.1) are (effectively) percentage departures from an expectation of growth ( $G_t$ ). This is equivalent to using a time-dependent mean for standardizing ring widths. In contrast, indices computed from equation (3.20) are (effectively) percentages of the corridor width ( $G2_t - G1_t$ )

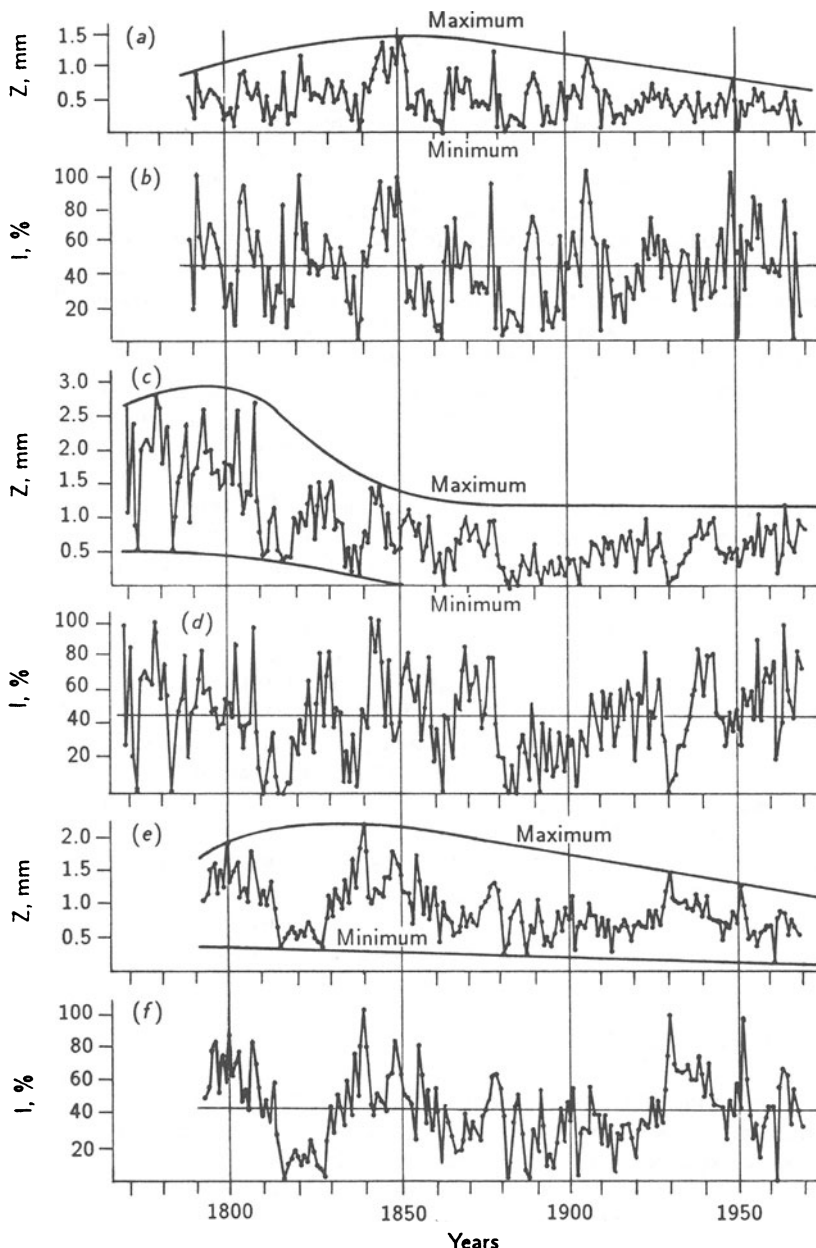


**Figure 3.8.** Examples of the corridor method of tree-ring standardization. The curves of maximum and minimum possible growth, which define the corridor, are shown for three Siberian larch (*Larix sibirica*) ring-width series [(a), (c), and (e)]. The standardized tree-ring indices derived from their respective corridors and equation (3.20) in the text are shown [(b), (d), and (f)].

$G1_t$ ), which is equivalent to using a time-dependent range for standardizing ring widths.

Whether one selects the mean or the range may affect the limits that the resultant indices take. Indices computed by equation (3.1) are bound only by zero and have an unbound maximum. Although standardized tree-ring chronologies developed from equation (3.1) are usually normally distributed (Fritts, 1976), the lower bound means that the potential exists for a truncated or skewed probability distribution. In contrast, indices computed by equation (3.20) are bound by both the minimum and the maximum growth curves. If the minimum and maximum curves pass through an excessive number of ring widths, then the possibility exists for creating a probability distribution function of indices that is truncated at either or both ends of the distribution.

The corridor method also assumes that the time variations in the maxima and minima, which define the corridor, are principally biological in origin rather than climatic. This assumption follows from the way that the maximum (or minimum) values in the early and later segments of a ring-width series are constrained to be identical in indexed form, even though they may be quite different in absolute ring width. This constraint implicitly assumes that the growth-limiting factors owing to climate were identical for those years. Shiyatov (personal communication) notes that these issues are not likely to be problems in the mean-value function of corridor-indexed series because of the inherent between-tree variability of the ring widths used to define the corridors.

Figures 3.8(b), 3.8(c), and 3.8(f) show the resultant indices computed from the estimated corridors in Figure 3.8 and equation (3.20). It is clear that the technique produces indices having a stationary mean and homogeneous variance. Unlike indices computed from equation (3.1) that have an expected value of 1.0 or 100%, indices computed by the corridor method have an expected value of .5 or 50%. Shiyatov and Mazepa (1987) note that this difference can be eliminated simply by re-standardizing each corridor-indexed series using its long-term mean and equation (3.1).

The corridors shown in Figure 3.8 were drawn by hand and human judgment using a flexible ruler. However, Shiyatov and Mazepa (1987) note that the technique can also be solved mathematically. They describe an estimation procedure that should make the corridor method more objective and far easier to implement as a standardization option.

*Double-detrending.* Holmes *et al.* (1986) describe a two-stage detrending method that they call *double-detrending*. A deterministic growth-trend model, such as the negative exponential curve, first estimates the observed trend in ring width. The tree-ring indices are computed from this curve and then detrended a second time using a cubic-smoothing spline. The second detrending is meant to remove any residual growth trend that is not modeled by the deterministic curve.

Holmes *et al.* (1986) justified double-detrending by illustrating that the negative exponential curve can fit the highly variable, steeply descending juvenile portion of the ring-width trend better than the less variable, flatter portion associated with maturity and old age. This is a consequence of least squares fitting, which can be dominated by the high-variance, juvenile portion of ring-width

series and of the inadequacy of the negative exponential curve as a model for the observed growth trend. In such cases, the outer portion of a ring-width series may be systematically underfit or overfit for decades. Holmes *et al.* (1986) also showed that a stiff spline fit alone to the same series by the 67% $n$  criterion was not sufficiently flexible to track the sharp curvature of the juvenile portion of the growth trend, even though it was quite adequate for the mature phase of the trend. Since each method of detrending was better for different portions of the growth trend, Holmes *et al.* (1986) reasoned that the sequential use of both techniques would correct the deficiencies of each method.

Cook (1985) examined the spectral properties of double-detrending and found that linear or negative exponential detrending followed by 67% $n$  spline detrending worked well without removing too much low-frequency variance.

### 3.3.5. Concluding remarks on growth-trend estimation

The estimation and removal of growth trends from tree-ring series should be based, as much as possible, on the intended application of the tree-ring data. This means that there should be an *a priori* expectation of what the signal of interest is in the ring-width measurements. Given this expectation, the method of detrending should be chosen that will reduce the low-frequency noise not associated with that signal. It is difficult to accomplish this task within an objective framework because of the uncertainty distinguishing signal from noise in a given ensemble of ring-width data. Inevitably, some assumptions must be made that may have a great effect on the final standardized tree-ring chronology. It is imperative that these assumptions are carefully considered and justified in any application of standardized tree rings.

In general, stochastic methods are preferable to deterministic methods because of the freedom that the former possess in fitting the behavior of ring widths as they are observed, not as theory would have them behave. However, the consequence of this added flexibility are the problems of *ad hoc* model selection and overfitting, which are more likely to occur for stochastic models than for deterministic models. There also seems to be some utility in using a hybrid double-detrending approach, which can compensate for local lack-of-fit problems of single detrending methods.

## 3.4. Estimation of the Mean Chronology

*E. Cook, S. Shiyatov, and V. Mazepa*

### 3.4.1. Introduction

Once a collection of ring-width series has been detrended and indexed into a new ensemble of tree-ring indices, the estimation of the common signal,  $C_t$ , can proceed. As mentioned earlier, tree-ring indices can be treated as stationary, stochastic processes that allow them to be treated as a collective ensemble of realizations containing both a common signal in the form of  $C_t$  (and perhaps  $D2_t$ ) and individual signals unique to the series ( $D1_t$  and  $E_t$ ).

### 3.4.2. Methods of computing the mean-value function

Three methods will be described that have been used in tree-ring studies: the arithmetic mean, the biweight robust mean that discounts outliers, and a mean based on testing for a mixture of normal distributions in the sample.

#### *The Arithmetic Mean*

The classical method of estimating  $C_t$  is by averaging the ensemble of detrended tree-ring indices across series for each year using the arithmetic mean (Fritts, 1976). This produces a time series mean-value function that concentrates the signal ( $C_t$ ) and averages out the noise ( $D_{1t}$  and  $E_t$ ). The arithmetic mean of  $m$  indices available in year  $t$  is computed as

$$\bar{I}_t = \sum_{j=1}^m I_j/m . \quad (3.21)$$

This is an estimate of the signal in the tree-ring indices for year  $t$ . The variance or spread of the frequency distribution of  $m$  indices about the mean is computed as

$$S_t^2 = \sum_{j=1}^m (I_j - \bar{I}_t)^2 / (m - 1) . \quad (3.22)$$

The square root of  $S_t^2$  is the standard deviation of  $m$  indices for year  $t$ . And, the variance of the mean, which is a measure of the noise or uncertainty in the estimation of the mean, is computed as

$$S_{\bar{I}}^2 = S_t^2 / m . \quad (3.23)$$

The square root of equation (3.23) is the standard error of the mean. These statistics are described in virtually all basic statistics textbooks and in Fritts (1976). A measure of the strength of the resultant estimate of  $C_t$  is the signal-to-noise ratio (SNR) (Wigley *et al.*, 1984; Briffa *et al.*, 1987), an estimate of which is given in equation (3.15). The SNR can only provide information about the quality of the observed signal, but says nothing about its relationship to the expected signal, which is not known at this stage (Briffa *et al.*, 1987).

#### *The Biweight Robust Mean*

Other more involved methods are available for computing the mean-value function. If there are suspected outliers, or extreme values, in the tree-ring indices, than a robust mean such as the biweight mean (Mosteller and Tukey, 1977) can

be used in place of the arithmetic mean. When outliers are present, the arithmetic mean is no longer a minimum variance estimate of the population mean, and it is not guaranteed to be unbiased. In contrast, robust means automatically discount the influence of outliers in the computation of the mean and, thus, reduce the variance and bias caused by the outliers. The use of a robust mean tacitly admits the likelihood of contamination by endogenous disturbance effects and other sources of noise having long-tailed, not normally distributed properties. Endogenous disturbance effects are likely to act as outliers because, as defined earlier, endogenous disturbances tend to behave as random events in space and time. The biweight mean for year  $t$  is computed by iteration as

$$\bar{I}_t^* = \sum_{j=1}^m w_t I_t , \quad (3.24)$$

where

$$w_t = \left[ 1 - \left( \frac{I_t - \bar{I}_t^*}{cS_t^*} \right)^2 \right]^2 ,$$

when

$$\left( \frac{I_t - \bar{I}_t^*}{cS_t^*} \right)^2 < 1 ,$$

otherwise 0. The weight function,  $w_t$ , is symmetric, and, therefore, unbiased in its estimation of central tendency when the data are symmetrically distributed (Cook, 1985).  $S_t^*$  is a robust measure of the standard deviation of the frequency distribution, which will be the median absolute deviation (MAD)

$$S_t^* = \text{median } \{|I_t - \bar{I}_t^*|\} , \quad (3.25)$$

and  $c$  is a constant, often taken as six or nine (Mosteller and Tukey, 1977). The constant  $c$  determines the point at which a discordant value is given a weight of zero. When this is the case, the outlier is totally discounted in computing the mean and, thus, has no influence on the estimation of the mean index. A constant  $c$  equal to 9 was used by Cook (1985) in developing a new tree-ring standardization procedure. From Mosteller and Tukey (1977),  $c$  equal to 9 is equivalent to totally rejecting any value exceeding  $\pm 6$  standard deviations from the mean, as estimated by equations (3.25) and (3.24), respectively. To start the iteration for computing the final  $\bar{I}_t^*$ , the arithmetic mean or median can be used as an initial estimate. Ordinarily, only three to four iterations are needed to

converge on an estimate of  $\bar{I}_t^*$  that does not change by more than  $10^{-3}$ . A robust estimate of the variance, analogous to equation (3.22), is also available for the biweight mean as

$$mS_{\bar{I}_t}^{*2} = \frac{m\Sigma'(I_t - \bar{I}_t^*)^2(1 - u_t^2)^4}{[\Sigma'(1 - u_t^2)(1 - 5u_t^2)][-1 + \Sigma'(1 - u_t^2)(1 - 5u_t^2)]} , \quad (3.26)$$

where  $u_t = (I_t - \bar{I}_t^*) / 9(\text{MAD})$  and  $\Sigma'$  indicates summation for  $u_t^2 \leq 1$ , only (Mosteller and Tukey, 1977). Similarly, a robust estimate of the variance of the biweight mean, analogous to equation (3.23), is also available as

$$S_{\bar{I}_t}^{*2} = \frac{\Sigma'(I_t - \bar{I}_t^*)^2(1 - u_t^2)^4}{[\Sigma'(1 - u_t^2)(1 - 5u_t^2)][-1 + \Sigma'(1 - u_t^2)(1 - 5u_t^2)]} , \quad (3.27)$$

where  $u_t$  and  $\Sigma'$  are defined as above.

Aside from its added computational complexity, the biweight mean has a potential cost or premium associated with it. When the sample of indices is devoid of outliers and approximates a Gaussian distribution, the variance of the biweight mean will be greater than that of the arithmetic mean. That is,

$$S_{\bar{I}_t}^{*2} > S_{\bar{I}_t}^2 .$$

This means that the biweight mean is less efficient in estimating the common signal when the assumed presence of outliers is false. However, when outliers are present in the sample, the variance of the biweight mean will be less than that of the arithmetic mean. That is,

$$S_{\bar{I}_t}^{*2} < S_{\bar{I}_t}^2 .$$

In this case, the biweight mean is more efficient at estimating the common signal. A measure of statistical efficiency of the biweight mean relative to the arithmetic mean is (Mosteller and Tukey, 1977)

$$\text{Efficiency} = S_{\bar{I}_t}^2 / S_{\bar{I}_t}^{*2} , \quad (3.28)$$

which is the ratio of the lowest variance feasible, under the Gaussian assumption, to the actual variance of the biweight mean. Under the Gaussian assumption and for moderate to large sample sizes (say  $m > 10$ ), the efficiency of the biweight mean exceeds 90% of the arithmetic mean. This is a small premium to pay for protection from outliers and is very difficult to see in practice. When the

sample size drops below 6, the simpler median can replace the biweight as the robust mean (Cook, 1985).

Extensive use of the biweight mean on closed-canopy forest tree-ring data (Cook, 1985) revealed that approximately 45% of the yearly means of 66 tree-ring chronologies showed some reduction in error variance using the biweight mean. This resulted in an average error variance reduction of about 20% in the robust mean-value functions compared with those based on the arithmetic mean. These results reveal the high level of outlier contamination in closed-canopy forest tree-ring data that can corrupt the estimated common signal if left unattended.

#### *Mean-Values from a Mixture of Normal Distributions*

Shiyatov and Mazepa (1987) and Mazepa (1982) describe another method of computing the mean-value function, which is based on examining the frequency distribution of the individual indices for each year. If the distribution is symmetrical and unimodal, the arithmetic mean is computed. However, if the distribution appears to be bimodal or multimodal, then the distribution is tested for a mixture of normal distributions. If mixed normal distributions are detected in the sample, then the mode of the grouping of largest indices is used as the best estimate of central tendency for that year. The selection of the grouping of largest indices is based on the notion that non-climatic effects, such as fruiting, will cause the ring widths of the affected trees to be narrower than the ring widths of the unaffected trees for the same years (Danilov, 1953; Kolischuk *et al.*, 1975). Therefore, the grouping of largest indices should more faithfully record the influence of climate.

In addition, the Law of Limiting Factors suggests that these anomalous effects are more likely to be seen when climate is less limiting to growth in a given year. That is, any expression of bimodality or multimodality in the sample distribution of tree-ring indices in a given year is more likely to be found when growth is not severely limited by climate. *Figure 9.9* shows six frequency histograms of tree-ring indices derived from Siberian larch (*Larix sibirica*) growing in the Ural Mountains, USSR. Four of the six examples show a clear indication of bimodality or multimodality, which tends to increase as the mean increases. The dispersion of the histograms increases as the mean level increases. This reflects the typical positive correlation between the means and standard deviations of tree-ring indices, which has been described by Fritts (1976).

*Figure 9.10* provides an illustration of the proposed technique of Shiyatov and Mazepa (1987). Because of the limited sample size for each year (usually < 30), Shiyatov and Mazepa (1987) restricted the test for mixtures of normal distributions to two distributions. The authors then tested four different tree-ring chronologies for climatic signal enhancement by modeling the climatic signal in each chronology after estimation by their new method and by the arithmetic mean alone. The percentage of years in which skewness or multimodality was indicated was approximately 25%. Shiyatov and Mazepa (1987) found a statistically significant ( $\alpha = .15$ ) increase in the strength of the modeled climatic signal in three of the four chronologies developed by their procedure. This encouraging

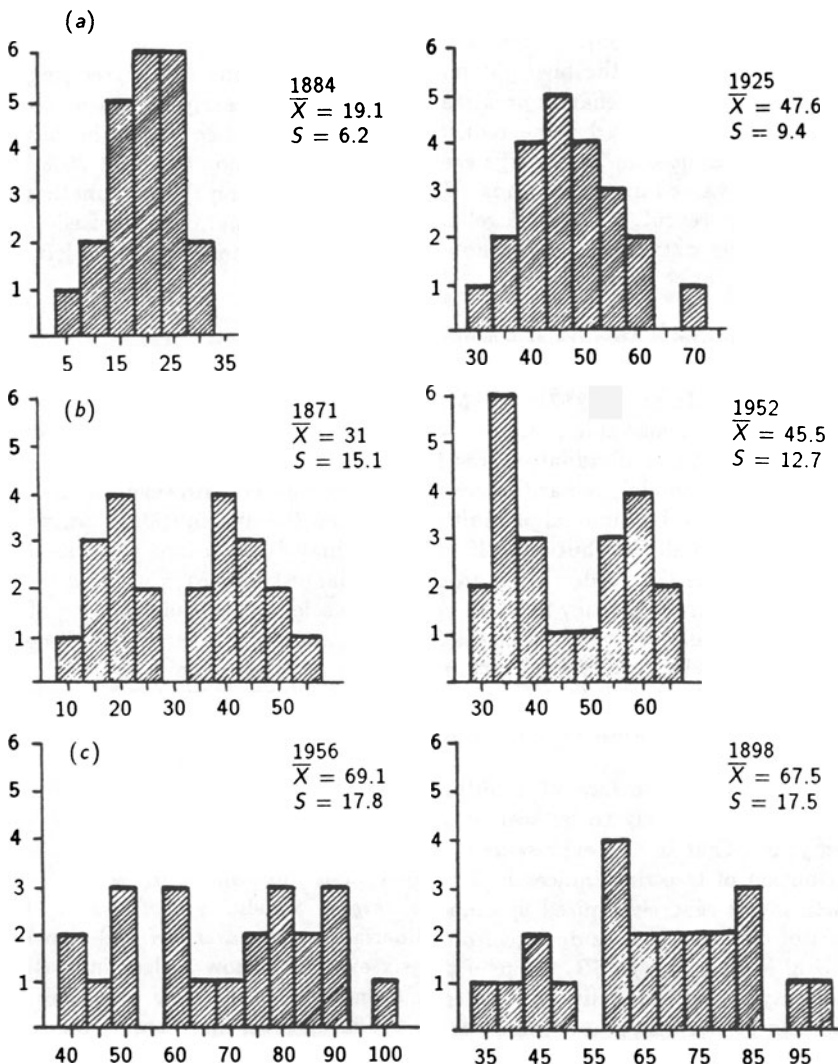
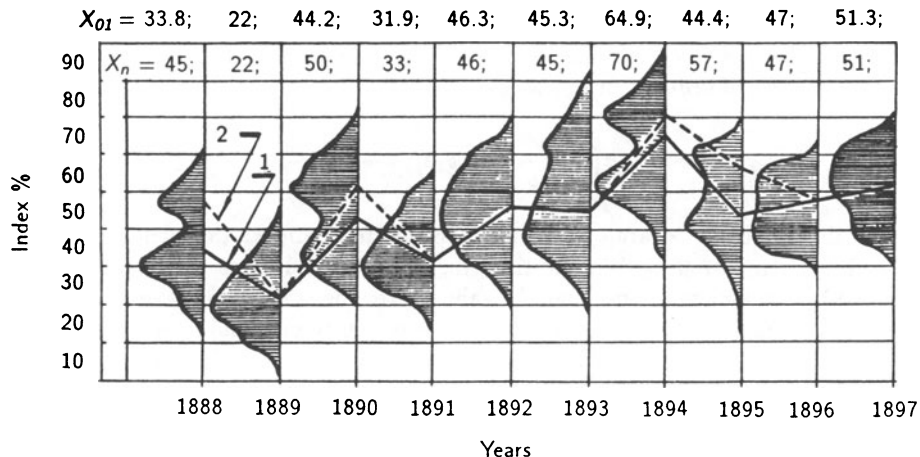


Figure 9.9. Some characteristic frequency distributions of *Larix sibirica* tree-ring indices for separate years. Note the clearly bimodal distributions in 9.9(b) and the more multimodal forms in 9.9(c).  $\bar{X}$  is the arithmetic mean, and  $S$  is the standard deviation for each distribution.

result is probably conservative because it is based on using all years, not just those years in which a mixture of normal distributions was detected.

As noted by Shiyatov and Mazepa (1987), their method has not yet dealt with the problem of serial dependence between the yearly sample distributions of indices and how it may affect any mixtures of normal distributions in each



**Figure 3.10.** An illustration of the method of computing the mean-value function based on modeling the distributions of sample indices as mixtures of normal distributions. The mean-value function is computed using the arithmetic mean of all samples (1); the mean-value function is computed by testing for the presence of a mixture of normal distributions and adjusting the estimate of the mean, accordingly (2). (From Shiyatov and Mazepa, 1987.)

sample. Therefore, further research is needed before the method can be routinely used for estimating mean-value functions. There is almost certainly some overlap between the expected performance of the biweight robust mean and the method of Shiyatov and Mazepa (1987). This performance overlap is likely when the frequency distribution is principally skewed or long-tailed, rather than bimodal or multimodal. When the former condition is present, either method may provide outlier-resistant measures of central tendency. However, when the latter condition occurs, the biweight mean will iterate toward the mode of highest frequency or to a compromise position between balanced modes, without regard to biological considerations. In this case, the performance of the two techniques will diverge.

### 3.4.3. The use of autoregressive-moving average models in estimating the common signal

The computation of the mean-value function, by any of the above methods, is easily done with the tree-ring indices. However, if the autocorrelation within each series is high, then a more statistically efficient estimate of the mean-value function (i.e., a higher SNR) is possible, in many cases, through the use of time series modeling and prewhitening techniques. Tree-ring series have an autocorrelation structure that allows the estimation of  $C_t$  to be broken down into a

two-stage procedure (Cook, 1985; Guiot, 1987a), based on ARMA time series modeling (Box and Jenkins, 1970).

Tree-ring indices can be expressed, in difference equation form, as an ARMA process of order  $p$  and  $q$ , viz.,

$$I_t = \phi_p I_{t-p} + \cdots + \phi_1 I_{t-1} + e_t - \theta_1 e_{t-1} - \cdots - \theta_q e_{t-q} , \quad (3.29)$$

where the values for  $e_t$  are serially random inputs or shocks that drive the tree-growth system as reflected in the tree rings, the  $\phi_i$  values are the  $p$  autoregressive (AR) coefficients, and the  $\theta_i$  values are the  $q$  moving average (MA) coefficients that produce the characteristic persistence or memory seen in the  $I_t$ . Equation (3.29) can be economically re-expressed in polynomial form using the backshift operator,  $B$ , as

$$I_t = [\theta(B)/\phi(B)] e_t , \quad (3.30)$$

where

$$\phi(B) = 1 - \phi_1 B - \cdots - \phi_p B^p$$

and

$$\theta(B) = 1 - \theta_1 B - \cdots - \theta_q B^q$$

(Box and Jenkins, 1970). On an individual series basis, the values for  $e_t$  are assumed to be composed of inputs owing to climate ( $C_t$ ) and those owing to disturbances and random variability ( $D1_t$  and  $E_t$ ). Component  $A_t$  is assumed to be nonexistent either in the raw ring-width series in total or for certain periods (Guiot, 1987a) (i.e.,  $I_t = R_t$ ), or to have been removed by detrending or differencing. Extensive ARMA modeling of tree-ring chronologies by Rose (1983) and Monserud (1986) indicates that western North American conifers are most commonly ARMA(1,1) processes, with the best competing models falling in the AR(1)-AR(3) classes. Cook (1985) restricted his analyses of eastern North American conifer and hardwood tree-ring chronologies to the AR process and found that AR(1)-AR(3) models were satisfactory, in most cases.

ARMA processes are examples of causal feedback-feedforward filters (Robinson and Treit, 1980) that are used extensively in geophysical signal analysis. The AR part of the process operates as a feedback filter, while the MA part operates as a feedforward filter. That is, the current  $I_t$  is a product of the current  $e_t$  plus past  $I_{t-i}$  inputs, which are fed back into the process, and past  $e_{t-i}$  inputs, which are fed forward upon the arrival of the current  $e_t$ . In this way, the potential for current growth is largely affected by previous radial growth ( $I_{t-i}$ ) and by reflections of antecedent environmental inputs ( $e_{t-i}$ ).

Thus, the ARMA process is an elegant mathematical expression of *physiological preconditioning* (Fritts, 1976).

An important concept of ARMA processes is the way in which they can operate as signal amplifiers. The amplifier mechanism can be seen in the variance formula of AR( $p$ ) processes, *viz.*,

$$\sigma_y^2 = \frac{\sigma_e^2}{1 - \rho_1\phi_1 - \rho_2\phi_2 - \cdots - \rho_p\phi_p} , \quad (3.31)$$

where  $\sigma_y^2$  is the variance of the observed AR process,  $\sigma_e^2$  is the variance of the unobserved random shocks, and  $\rho_i$  and  $\phi_i$  are the theoretical autocorrelation and autoregression coefficients of the process. If both the  $\rho_i$  and  $\phi_i$  are positive, which is usually the case for tree-ring indices, then  $\sigma_y^2$  will always be greater than  $\sigma_e^2$ . A reflection of this amplifier mechanism is transience. That is, the effect of a given  $e_t$  in a tree-ring series, whether climatic or from disturbance, will last for several years or, in extreme cases, decades before it disappears (Cook, 1985). The consequence of transience, when endogenous disturbance shocks are present in the  $e_t$ , is a degradation of the SNR of the  $C_t$  in the mean-value function of tree-ring indices.

To remove the effects of unwanted, disturbance-related transience on the common signal among trees, the tree-ring indices can be modeled and prewhitened as AR( $p$ ) (Cook, 1985) or ARMA( $p, q$ ) (Guiot, 1987a) processes before the mean-value function is computed. The order of the process can be determined at the time of estimation using the Akaike Information Criterion (AIC) (Akaike, 1974). Once the ARMA( $p, q$ ) coefficients are estimated, the prewhitening is carried out as

$$e_t = I_t - \phi_1 I_{t-1} - \cdots - \phi_p I_{t-p} + \theta_1 e_{t-1} + \cdots + \theta_q e_{t-q} \quad (3.32)$$

in difference equation form, or

$$e_t = [\phi(B)/\theta(B)] I_t \quad (3.33)$$

in backshift operator form. The tree-ring series are now *white noise*.

The resulting  $e_t$  represent the contributions of  $C_t$ ,  $D1_t$ , and  $E_t$ , with  $D2_t$  assumed to be absent at this stage. The reduction of the transient effects of endogenous disturbance pulses results in an increase in fractional common variance (Wigley *et al.*, 1984) or %Y (Fritts, 1976) and in an improved SNR in the mean-value function of the  $e_t$ , denoted  $e_t$ . This results in an improved estimate of  $C_t$ , especially if the biweight robust mean is also used in computing  $e_t$ . Cook (1985) found that the average absolute increase in fractional common variance between sampled trees was about 7% for 66 tree-ring chronologies developed from closed-canopy forest stands. The average relative increase in fractional common variance, compared with that of a mean-value function developed

without using AR modeling, was about 25%. There are no comparable figures for ARMA-based models.

The estimate of  $C_t$ , in the form of  $e_t$ , is incomplete because it is missing the natural persistence owing to climate and tree physiology. To have a complete model of the common signal within the ensemble, an estimate of the common persistence structure among all detrended tree-ring series is necessary. For the pure AR model, a pooled estimate of autoregression, denoted  $\Phi(B)$ , can be computed directly from lag-product sum matrices of the ensemble that include information on persistence both within and among series (Cook, 1985). The method appears to be quite robust in the face of high levels of out-of-phase fluctuations among series that are caused by endogenous disturbances. Unfortunately, this pooling procedure is difficult to apply to the ARMA case because of the highly nonlinear MA coefficients.

Guiot (1987a) addressed the estimation of the common ARMA model by first creating a mean-value function of raw ring-width series from very old trees, which were selected by principal components and cluster analysis of the corresponding white-noise series. The common ARMA( $p, q$ ) model, denoted  $\Theta(B)/\Phi(B)$ , was then estimated for stationary subperiods in the mean ring-width series. However, this approach may be difficult to apply to the general closed-canopy forest where stationary subperiods rarely exist for any length of time (e.g., Figures 3.1 and 3.2). As an alternative, the ring-width series could be detrended first, a robust mean-value function created, and the mean series modeled as an ARMA process to produce  $\Theta(B)/\Phi(B)$ . This method would depend upon sufficient replication to diminish the effects of endogenous disturbance effects. Experiments in detrending ring-width series (Cook, 1985) indicate that the choice of the detrending method will have little effect on the order and coefficients of the mean ARMA process as long as the variance removed by the trend line is effectively all trend, as defined by Granger (1966).

The estimation of the common signal components is now complete. A final tree-ring chronology,  $I_t$ , containing both common signal components, can be easily created by simply convolving the pooled AR,  $\Phi(B)$ , or the ARMA [ $\Theta(B)/\Phi(B)$ ] operators with the  $e_t$  (Cook, 1985; Guiot, 1987a), once suitable starting values are obtained. The  $q$  starting values for the MA component will ordinarily be set to zero, the unconditional expected value of  $e_t$ . The  $p$  starting values for the AR component may be obtained from the  $I_t$  lost through prewhitening (Cook, 1985), by back-forecasting of the  $I_t$  past the beginning of the  $I_t$  (Box and Jenkins, 1970), or by using the unconditional expected value of the  $I_t$ . If the characteristic transience of the AR component decays rapidly, then the choice of starting values will have little effect on the final series.

For the full ARMA case, the final estimate of  $C_t$  is

$$I_t = [\Theta(B)/\Phi(B)] e_t . \quad (3.34)$$

Aside from producing an efficient estimate of  $C_t$ , knowledge of  $[\Theta(B)/\Phi(B)]$  and  $e_t$  are also useful for estimating  $D1_t$  and  $E_t$  in the individual tree-ring series.

### 3.5. Correcting for Trend in Variance Due to Changing Sample Size *S. Shiyatov, V. Mazepa, and E. Cook*

With the possible exception of tree-ring chronologies developed from even-aged stands or narrow-age classes of trees, the yearly sample size of  $m$  indices in a tree-ring chronology can be expected to diminish backward in time as younger trees drop out of the series. As the sample size decreases below some threshold, commonly between 5 and 10, a perceptible increase in the variance of the mean-value function can be discerned when compared with better replicated time intervals. This increase in variance is largely a function of decreasing sample size, which is independent of changes in the variance owing to environmental influences on radial growth. This problem of nonuniform variance owing to changing sample size was recognized by Schulman (1956). He suggested deleting the early, poorly replicated portions of chronologies because of this non-climatic, statistical artifact. To date, this method of deletion is commonly used in dendro-climatic studies to avoid spurious conclusions concerning past climatic variability.

The change in time series variance, described above, is related to the change in variance of the arithmetic mean, equation (3.23), which is proportional to  $1/m$ . As  $m$  gets small (say,  $m < 10$ ), additional reductions in  $m$  result in rapid increases in  $1/m$ . The change in the standard error of the mean, square root of equation (3.23), is even more dramatic because it is proportional to  $1/\sqrt{m}$ . How quickly this effect will manifest itself in the mean-value function will depend upon the variance of the sample of  $m$  indices, equation (3.22), and the signal-to-noise ratio (SNR) of the chronology, equation (3.15). The SNR and a related measure called the subsample signal strength (SSS) (Wigley *et al.*, 1984) will be described in more detail in Section 3.6. As will be shown, SSS can be used to determine the point in time where a chronology loses too much accuracy to be useful, owing to reduced sample size. For now, it is sufficient to illustrate the sample-size effect on the variance of tree-ring chronologies and describe a method developed by Shiyatov and Mazepa (1987) for correcting this effect.

*Figure 3.11* (Shiyatov and Mazepa, 1987) shows the way in which the coefficient of variation of a tree-ring chronology can vary as a function of sample size. These plots were created, from an ensemble of 22 indexed *Picea obovata* tree-ring series, by randomly selecting many subsets of size  $m = 1 - 20$  from the total and by computing the coefficient of variation of each mean series. Below about  $m = 7$ , there is a clear increase in the plots of the mean and maximum coefficients of variation. This reflects the increase in variance owing to decreasing sample size. The plot of minima remains much more constant in the range of  $m = 2 - 10$ . This probably reflects a subset of series in the ensemble that are highly correlated and, therefore, have high SNR. Nonetheless, *Figure 3.11* indicates that a trend in variance from decreasing sample size should be expected most of the time.

Shiyatov and Mazepa (1987) note that there are times when it is important to use as much of a tree-ring chronology as possible. Given this circumstance, they suggest the following method for correcting the trend in variance caused by

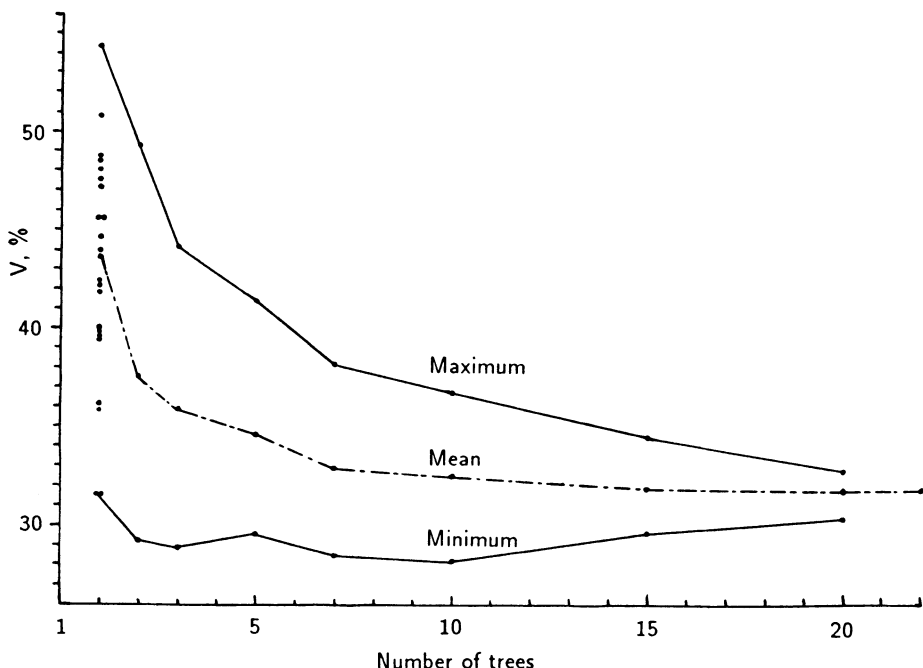


Figure 3.11. The maximum, mean, and minimum values of the coefficient of variation (CV) obtained from a different number of sampled *Picea obovata* trees from the same site. The dots (·) on the left of the chart indicate the range of the CV of the individual series.

changing sample size. For the time interval of maximum sample size,  $m_{\max}$ , compute the coefficient of variation for the mean series as

$$CV_{std} = s_{std}/\bar{x}_{std} \quad , \quad (3.35)$$

where  $s_{std}$  and  $\bar{x}_{std}$  are the standard deviation and mean, respectively, of that series.  $CV_{std}$  is the standard used for contracting the variance in other time periods having smaller sample sizes. Having estimated  $CV_{std}$ , new coefficients of variation  $CV_k$  are then computed using equation (3.35) for the total time period of the longest series, the entire period of overlap of the mean of the two oldest series, the entire period of overlap of the mean of the three oldest series, and so on up to the time interval and sample size covered by  $CV_{std}$ . The variance corrections for the time intervals not having maximum sample size are then computed as

$$I_t^{cor} = (I_t^{act} - I) * k + I \quad , \quad (3.36)$$

where  $I_t^{\text{cor}}$  is the corrected tree-ring index,  $I_t^{\text{act}}$  is the uncorrected index for year  $t$ ,  $I$  is the mean of the entire mean series, and  $k$  is the coefficient of contraction estimated as  $k = \text{CV}_{\text{std}}/\text{CV}_k$ , which is the ratio of the coefficient of variation of the  $m_{\text{max}}$  time period to that for a sample size  $m < m_{\text{max}}$ .

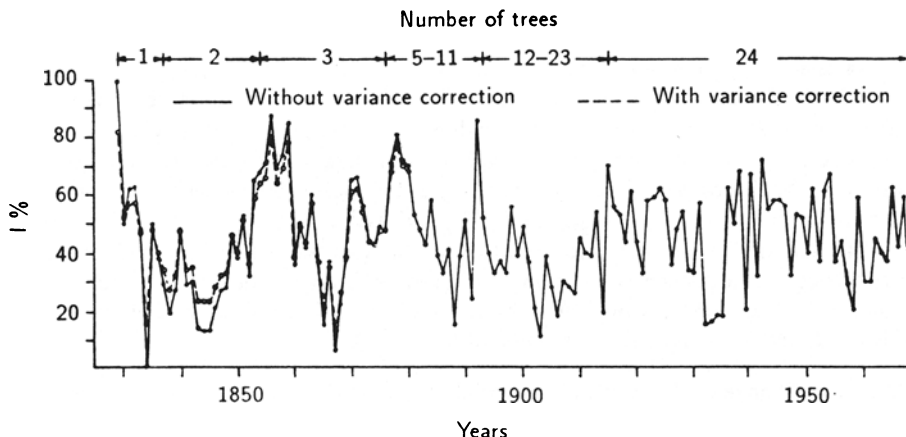
Table 9.2 shows the way in which  $\text{CV}_k$  varies in an ensemble of tree-ring indices of 24 *Picea obovata*. The last value for all sampled trees is  $\text{CV}_{\text{std}}$ . These values reinforce the example in Figure 9.11 and, again, indicate that sample-size effects on variance are likely to occur at some point below  $m = 10$ . Having estimated the necessary  $\text{CV}_{\text{std}}$  and  $\text{CV}_k$  in Table 9.2, Shiyatov and Mazepa (1987) used this information in equation (3.36) to produce a corrected tree-ring chronology. The uncorrected and corrected series are shown in Figure 9.12. There is a clear contraction in the variance of the corrected series below  $m = 5$ , in accordance with the values in Table 9.2.

Table 9.2. Change in the coefficient of variation (CV) of a mean chronology (*Picea obovata*) owing to changing sample size. The % deviation of each CV from the standard value is used to correct variance of the mean series for changing sample size.

Sample size	Time interval	Years	CV in %	% Deviation of CV from the standard
1	1829–1968	140	58.5	+20.3
2	1837–1968	132	57.2	+19.0
3	1854–1968	115	49.9	+11.7
5	1876–1968	93	46.0	+7.8
6	1878–1968	91	43.6	+5.4
7	1879–1968	90	42.4	+4.2
8	1881–1968	88	41.2	+3.0
9	1882–1968	87	39.5	+1.3
10	1884–1968	85	38.4	+0.2
11	1885–1968	84	38.8	+0.6
12	1893–1968	76	37.1	-1.1
<i>All sampled trees – The standard</i>				
13–24	1894–1968	75	38.2	0.0

A trend in variance, which is independent of changing sample size, can also be expected in tree-ring chronologies of ring-porous tree species, such as *Quercus*. The active xylem vessels of ring-porous species are almost totally restricted to the newly formed vessels of each growing season. These large *springwood* vessels are formed from stored carbohydrates before the flush of new leaves each year. Their contribution to each total ring width varies little from year to year, compared with the subsequently formed *summerwood* vessels, and declines more slowly with age than the summerwood width. Thus, the contribution of springwood vessels to the total ring width often increases with age. This causes the yearly variance of ring-porous radial increments to decrease with age in a way that is independent of sample size.

As a means of correcting this problem in *Quercus* tree-ring chronologies, Cook (unpublished) included in the tree-ring standardization program ARSTND



**Figure 8.12.** The mean chronology of 24 *Picea obovata* tree-ring series without (solid line) and with (dashed line) the variance correction based on the coefficient of variation. The change in sample size in the chronology is indicated by the number of trees at the top of the plot. The most obvious contraction of variance occurs below a sample size of five trees.

(Cook and Holmes, n.d.) an option for removing the trend in variance in tree-ring chronologies. This method is distinctly different from that of Shiyatov and Mazepa (1987) and does not rely on the coefficient of variation. It is based on fitting a smoothing spline to the absolute values of the mean-corrected, standardized tree-ring indices. The spline is used to track the trend in the standard deviation of the indices, as revealed by the low-frequency fluctuations in the absolute values. Each absolute value is divided by its respective spline value. The corrected absolute values are then back-transformed into normal tree-ring indices and scaled to have the same overall variance as the original, uncorrected indices. This technique can be used on both single series and the mean-value function. In the latter case, it will correct for both the trend in variance caused by ring-porous wood anatomy and the changing sample size, if the variance correction is not made on the individual series.

Given that the method of Shiyatov and Mazepa (1987) or the method in the *ARSTND* program (Cook and Holmes, n.d.) can be used to correct for a trend in variance owing to changing sample size, a word of caution must be made. The increase in variance when  $m$  gets small is a consequence of the noise in the ensemble that is not adequately reduced by averaging. As a result, those mean values based on small  $m$  are considerably less precise and probably less accurate than the mean indices derived from larger sample sizes. Correcting the variance for changing sample size will not necessarily improve the accuracy. It merely adjusts those means based on  $m < m_{\max}$  to behave as if they were based on the maximum sample size. As a consequence, the loss of accuracy is masked by the variance correction. Additional information on the accuracy of the small

$m$  segment of tree-ring chronologies can be obtained by computing the SSS (sub-sample signal strength) and should be made available if corrections are made to the variance for changing sample size.

### 3.6. Basic Chronology Statistics and Assessment

*K. Briffa and P.D. Jones*

#### 3.6.1. Measuring the statistical quality of a chronology

This section is concerned with the problem of assessing the statistical confidence of a chronology. Up to this point we have described various approaches and techniques that are used to produce tree-ring chronologies from such variables as ring widths or maximum latewood density data. We have discussed in some detail the ways in which measured series of these data may be standardized during chronology production so that the unwanted index time series, thought to obscure those variations representing the hypothesized forcing with which we are concerned, has been removed. In other words, we have described the production of chronologies in terms of a noise-reduction process, and the concepts of signal and noise have been clearly framed in terms of specific hypotheses or applications.

Here, we will investigate the concept of a chronology signal. This signal is a statistical quantity representing the common variability present in all of the tree-ring series at a particular site. The strength of this signal is estimated empirically, and here it is not necessary to speculate on the forcing(s) of which the signal is the manifestation. We merely assume that a group of tree-ring series from a site make up one sample from a hypothetical population whose average would be the *perfect* chronology – one that fully represents the underlying forcing(s). The variance of any series of tree-ring indices will contain this common forcing signal (though it will be modified according to how the data are standardized), but in any one core it will be obscured by variability common only to the specific tree and core – the statistical noise. By definition, this noise is uncorrelated from core to core and, therefore, will cancel out in a chronology to an extent that depends on the number of series being averaged. Therefore, the question of the statistical quality of a chronology may be phrased as follows: To what degree does the chronology represent the hypothetical population chronology? To answer this question, it is necessary, first, to estimate the strength of the signal and, second, to quantify how clearly this signal is expressed in the chronology. We shall discuss these points in turn.

#### 3.6.2. Estimating the chronology signal strength

##### *The Analysis of Variance Technique*

Traditionally, dendroclimatologists have used the Analysis of Variance (ANOVA) technique to estimate signal and noise within groups of standardized

tree-ring series (indices) by measuring common variability within and between trees. Considered sampling design also allows the dendrochronologist to judge the relative importance of various environmental influences acting on the growth of trees. A discussion of this use of ANOVA can be found in Fritts (1976).

*Table 3.3* (Fritts, 1976) illustrates how the relative importance of within-tree and between-tree signals is calculated by computing the variance components,  $V(Y)$ , etc., associated with specific groups of standardized series that make up the final chronology. In this example, the analysis involves indices  $Y_{ijk}$ , where  $i = 1$  to  $t$  trees, each with  $j = 1$  to  $c$  cores (hence, the total number of cores is

$$C = \sum_{i=1}^t c_i .$$

All data series run from  $k = 1$  to  $n$  years. The various fractional variance components are calculated as shown in *Table 3.3*.

The fractional variance component for the chronology,  $V(Y)$ , according to Fritts (1976), shows how much of the variance is common among all trees and cores. This, he says, represents the overall growth forcing(s) at the site and, as such, it is a measure of the chronology signal.

The component *chronologies of trees*,  $V(YT)$ , measures that part of the overall variance that is common to cores within trees but not common between trees. This is the between-tree noise. The *chronologies of cores within trees* component,  $V(YCT)$ , is a measure of the variance not common among individual cores within any one tree, the within-tree noise. Subtracting this value from 1, therefore, defines the within-tree signal.

#### *The Mean Correlation Technique and a New Definition of the Chronology Signal*

When producing a chronology of a tree-ring variable, it is a simple matter to calculate a correlation matrix displaying the relationships between all series of indices for individual cores. Given such a matrix, several mean correlation values can be calculated. This represents an alternative approach to estimating the quantities that arise in the ANOVA.

First, we should define the correlation matrix grand mean, i.e., the mean of all correlations among different cores – both within and between trees. This can be termed

$$\bar{r}_{\text{tot}} = \frac{1}{N_{\text{tot}}} \sum_{i=1}^t \sum_{\substack{l=i \\ i \neq l}}^t \sum_{j=1}^{c_i} r_{ij} , \quad (3.37)$$

where

$$N_{\text{tot}} = \frac{1}{2} \left( \sum_{i=1}^t c_i \right) \left[ \left( \sum_{i=1}^t c_i \right) - 1 \right] .$$

An estimate of the within-tree signal is given by averaging the correlation coefficients between series of indices from the same tree over all trees. This within-tree signal can be denoted as

$$\bar{r}_{wt} = \frac{1}{N_{wt}} \sum_{i=1}^t \left( \sum_{j=2}^{c_i} r_{ij} \right) , \quad (3.38a)$$

where

$$N_{wt} = \sum_{i=1}^t \frac{1}{2} c_i(c_i - 1) . \quad (3.38b)$$

The expression  $1 - \bar{r}_{wt}$  is equivalent to  $V(YCT)$  in *Table 3.3*.

We can also calculate a between-tree signal,  $\bar{r}_{bt}$ , defined as the mean inter-series correlation calculated between all possible pairs of indexed series drawn from different trees:

$$\bar{r}_{bt} = \frac{1}{N_{bt}} (\bar{r}_{tot} N_{tot} - \bar{r}_{wt} N_{wt}) , \quad (3.39a)$$

where

$$N_{bt} = N_{tot} - N_{wt} . \quad (3.39b)$$

Fritts (1976, page 294) noted, using empirical evidence, that  $V(Y)$  defined in *Table 3.3* is invariably close to  $\bar{r}_{bt}$ . Wigley *et al.* (1984) have shown that  $V(Y)$  and  $\bar{r}_{bt}$  are in fact identical provided that both estimates are calculated using data normalized over the common period of analysis. The normalization of individual series of indices is not common practice in chronology development. However, both the ANOVA and correlation approaches to estimating chronology-population signals tacitly assume that there is no difference between the means of individual core series. Generally, standardization ensures that there is little difference. If, however, each indexed series is normalized over its whole length prior to averaging, then this generally ensures that the means of the core indices over the common period are not significantly different from zero [i.e., that  $V(YC)$  is very close to zero]. This is recommended. The between-tree noise,  $V(YT)$  in *Table 3.3*, is conveniently calculated as the difference between  $\bar{r}_{wt}$  and  $\bar{r}_{bt}$ .

Wigley *et al.* (1984) derived the relationship between  $\bar{r}_{bt}$  and  $V(Y)$  using data from only one core per tree and confirmed the result empirically. In fact,  $\bar{r}_{bt}$  defined by equation (3.39a) and  $V(Y)$  in *Table 3.3* are also equivalent for multiple cores per tree (identical if the data are normalized over the common

**Table 3.9.** Analysis of variance table showing how the different sources of chronology variation are calculated. Equivalent mean correlation values described in the text are also shown. ANOVA table adapted from Fritts (1976).

Variance source	Corrected sum of squares	Degrees of freedom
Core class means	$\frac{1}{tn} \left[ \sum_{j=1}^c \left( \sum_{i=1}^t \sum_{k=1}^n Y_{ijk} \right)^2 \right] - K = C$	$(c - 1)$
Tree means	$\frac{1}{cn} \left[ \sum_{i=1}^t \left( \sum_{j=1}^c \sum_{k=1}^n Y_{ijk} \right)^2 \right] - K = T$	$(t - 1)$
Core means with trees	$\frac{1}{n} \left[ \sum_{i=1}^t \sum_{j=1}^c \left( \sum_{k=1}^n Y_{ijk} \right)^2 \right] - C - \frac{T}{K} = CT$	$(c - 1)(t - 1)$
Mean indices in chronology	$\frac{1}{tc} \left[ \sum_{k=1}^n \left( \sum_{i=1}^t \sum_{j=1}^c Y_{ijk} \right)^2 \right] - K = Y$	$(n - 1)$
Chronologies of trees	$\frac{1}{c} \left[ \sum_{k=1}^n \sum_{i=1}^t \left( \sum_{j=1}^c Y_{ijk} \right)^2 \right] - Y - \frac{T}{K} = YT$	$(n - 1)(t - 1)$
Chronologies of core classes	$\frac{1}{t} \left[ \sum_{k=1}^n \sum_{j=1}^c \left( \sum_{i=1}^t Y_{ijk} \right)^2 \right] - Y - \frac{C}{K} = YC$	$(n - 1)(c - 1)$
Chronologies of cores with trees	$\left[ \sum_{k=1}^n \sum_{i=1}^t \sum_{j=1}^c \left( Y_{ijk} \right)^2 \right] - Y - C - \frac{CT}{K} - YC - YT = YCT - K$	$(n - 1)(c - 1)(t - 1)$

Table 3.3. Continued.

Variance source	Mean square	Variance component	Fractional variance component	Equivalent mean correlation
Core class means	$MS(C) = \frac{C}{(c-1)}$			
Tree means	$MS(T) = \frac{T}{(t-1)}$			
Core means with trees	$MS(CT) = \frac{CT}{(t-1)(c-1)}$			
Mean indices in chronology	$MS(Y) = \frac{Y}{(n-1)}$	$\frac{MS(Y) - MS(YT)}{ct} = V\{Y\}$	$\frac{V(Y)}{\text{Total } V} = V\{Y\}$	$r_{bt}$
Chronologies of trees	$MS(YT) = \frac{YT}{(n-1)(t-1)}$	$\frac{MS(YT) - MS(YCT)}{c} = V\{YT\}$	$\frac{V(YT)}{\text{Total } V} = V\{YT\}$	$r_{wt} - r_{bt}$
Chronologies of core classes	$MS(YC) = \frac{YC}{(n-1)(c-1)}$	$\frac{MS(YC) - MS(YCT)}{t} = V\{YC\}$	$\frac{V(YC)}{\text{Total } V} = V\{YC\}$	Zero
Chronologies of cores with trees	$MS(YCT) = \frac{YCT}{(n-1)(c-1)(t-1)}$	$MS(YCT) = V(YCT)$	$\frac{V(YCT)}{\text{Total } V} = V\{YCT\}$	$1 - r_{wt}$
The correction factor, $K = \frac{1}{tcn} \left[ \sum_{i=1}^t \sum_{j=1}^c \sum_{k=1}^n Y_{ijk} \right]^2$		where $i = 1, 2, \dots, t$ $j = 1, 2, \dots, c$ $k = 1, 2, \dots, n$	$t = \text{number of trees}$ $c = \text{number of cores per tree}$ $n = \text{number of years}$	
Total $V = V\{Y\} + V\{YT\} + V\{YC\} + V\{YCT\}$				

period). However,  $\bar{r}_{bt}$  is not the best estimate of the chronology signal where more than one core series per tree are involved. Though  $V(Y)$  (and the equivalent  $\bar{r}_{bt}$ ) is commonly used to represent the chronology signal, it is not an ideal measure of the forcing that is common between and within all trees at a site. This is because  $V(Y)$  incorporates noise associated with differences among cores within trees – noise that is reduced by averaging. It is possible to define a chronology signal that makes allowance for this.

In seeking to generalize the results of their paper, Wigley *et al.* (1984, page 211) stated:

Our analysis only considers the case of one core per tree but it can be adapted to more general cases. For example, multiple cores may be averaged to produce a single time series for each tree, or  $\bar{r} \dots$  can be determined using only a single core per tree if the early parts of a chronology suggest that such a strategy is more appropriate.

The second option they suggest will give an estimate of  $\bar{r}_{bt}$  (and one which does not use all of the available data). Importantly, the potential for measuring the within-tree signal will be wasted. Their first suggestion, though it too does not give a value for  $\bar{r}_{wt}$ , gives a better estimate of the chronology signal, one that is less obscured by within-tree noise and involves calculating the mean correlation between series of previously averaged core series. We can denote this as  $\bar{r}_{mt}$ , the mean-tree correlation mean, i.e.,

$$\bar{r}_{mt} = \frac{2}{t(t-1)} \sum_{i=1}^t \sum_{\substack{l=1 \\ l \neq i}}^t r_i^* , \quad (3.40)$$

where  $r_i^*$  is the correlation coefficient between the mean of all core time series for tree  $i$  and the mean for tree  $i$ . It can be shown that  $\bar{r}_{mt}$  is given by

$$\bar{r}_{mt} = \frac{\bar{r}_{bt}}{\bar{r}_{wt} + \frac{1 - \bar{r}_{wt}}{c}} \quad (3.41)$$

where  $\bar{r}_{bt}$  is given by equation (3.39a),  $\bar{r}_{wt}$  is given by equation (3.38a), and  $c$  is the number of cores per tree and must be the same for all trees. If an unequal number of cores per tree are averaged, instead of  $c$ , an effective number of cores,  $c_{\text{eff}}$ , should be used such as

$$\frac{1}{c_{\text{eff}}} = \frac{1}{t} \sum_{i=1}^t \frac{1}{c_i} , \quad (3.42)$$

where  $t$  is the number of trees and  $c_i$  is the number of cores in tree  $i$ . Hence, we can define a chronology-signal estimate that incorporates both within- and between-tree signals, which we will call the effective chronology signal,  $\bar{r}_{\text{eff}}$ ,

$$\bar{r}_{\text{eff}} = \frac{\bar{r}_{bt}}{\bar{r}_{wt} + \frac{1 - \bar{r}_{wt}}{c_{\text{eff}}}} . \quad (3.43)$$

From this point on we will refer to  $\bar{r}_{\text{eff}}$ , but it should be remembered that, when studying the same number of cores per tree,  $\bar{r}_{\text{eff}}$  is equal to  $\bar{r}_{mt}$ . When the number of cores per tree are unequal, equation (3.43) gives a chronology-signal estimate that is still extremely close to the one derived from equation (3.40). As  $\bar{r}_{wt}$  has, by definition, a lower limit equal to  $\bar{r}_{bt}$  it can be shown that equation (3.43) gives a measure of the chronology signal that is almost invariably greater than  $\bar{r}_{bt}$  and implies that, to date, the strength of common forcing has been generally underestimated by quoting chronology  $V(Y)$  or  $\bar{r}_{bt}$  values. Figure 3.19 illustrates how the degree of underestimation depends on  $\bar{r}_{bt}$  and  $\bar{r}_{wt}$ . If as an example we say that  $\bar{r}_{wt}$  is often in the range 0.6–0.7 and chronologies often comprise two cores per tree, the  $\bar{r}_{\text{eff}}$  value for the chronology signal may well be 20% to 30% greater than the  $\bar{r}_{bt}$  value. The difference is less where  $\bar{r}_{wt}$  is higher and greater where it is lower. The difference is also less marked when  $\bar{r}_{wt}$  values are based on more cores per tree.

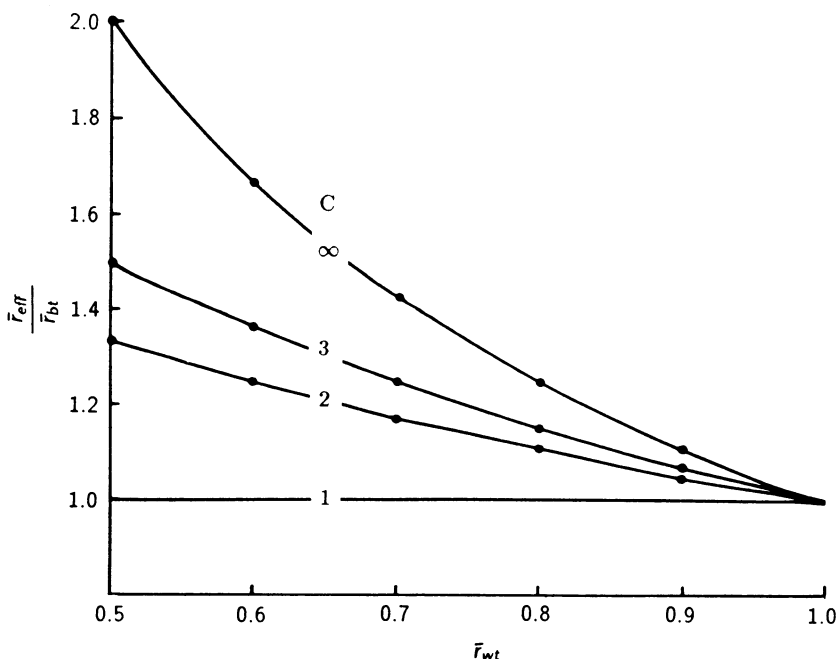


Figure 3.19. The ratio of  $\bar{r}_{\text{eff}}$  and  $\bar{r}_{bt}$  plotted as a function of  $\bar{r}_{wt}$  and the number of cores per tree,  $c$ .

### *Relative Advantages of the Correlation Versus the ANOVA Method*

As generally implemented, the ANOVA requires that all series must span a common set of years and that each tree must be represented by the same number of cores. Restrictions, such as trees of different ages or core samples of unequal numbers, may limit the period of analysis when using ANOVA or they might necessitate the exclusion of a number of cores from the analysis. In extreme cases, there might not be a common overlap of sufficient length in the series to make a useful analysis.

An advantage of the correlation-based technique is that it allows all series of indices to be used, including the case where the number of series varies from tree to tree. Furthermore, it is not necessary for all of the series to have a common period of overlap. A correlation matrix can be computed using the maximum overlap period between each pair of series and the signal parameters estimated from this. (In practice, one would set a minimum limit on the length of the overlap required to calculate a correlation coefficient, e.g., 30 years.)

### *Illustrative Examples*

*Table 3.4* gives some examples of the calculation of the quantities discussed above. In this simplified illustration, two correlation matrices are shown – each involving four trees: two with two cores, one with a single core, and one with three cores. (These numbers are in fact taken from the full correlation matrix of data for the chronology *Twisted Tree-Heartrot Hill* described in Section 3.7. The data used here have been standardized using the modified negative exponential option.) The top matrix is calculated over the overall common period, 1807–1974. The mean of the values without a footnote is the between-tree signal,  $\bar{r}_{bt}$ , [ $V(Y)$  in *Table 3.9*] and is 0.39 in this case. The within-tree signal,  $\bar{r}_{wt}$ , is the mean of the values with a footnote, 0.76; the within-tree noise,  $V(YCT)$ , is given by subtracting  $\bar{r}_{wt}$  from 1 to give 0.24. The between-tree noise,  $V(YT)$ , calculated as the difference between  $\bar{r}_{wt}$  and  $\bar{r}_{bt}$ , is 0.37. The chronology signal,  $\bar{r}_{eff}$ , calculated using equation (3.43), is 0.43 for the top matrix. All of the values in the top matrix are based on a common 168-year period.

The lower matrix in *Table 3.4* is calculated using the maximum overlaps between individual pairs of series. These overlaps range from 205 to 463 years. Use of the values in this matrix gives a lower value of  $\bar{r}_{bt}$  of 0.30. The core-to-core variability of  $\bar{r}_{bt}$  is also reduced from a standard deviation of 0.21 to 0.12. The  $\bar{r}_{wt}$  value is very similar to the previous one at 0.77, but again it has a smaller standard deviation. The  $\bar{r}_{eff}$  value for this matrix is 0.33.

On this evidence the second matrix seems to give more conservative (i.e., lower) estimates of the signal parameters. Experiments have been made where very short-period correlations are excluded and where the mean correlations are computed by preferentially weighting those based on longer overlaps, but such modifications do not seem to affect the results significantly.

Both the ANOVA-derived and correlation-based signal estimates are unbiased estimates of the population parameters (Wigley *et al.*, 1984) and give

**Table 3.4.** Alternative correlation matrices for calculating the different signal estimates. The column and row headings identify the different tree (1st figure) and core (2nd figure) series, i.e., 4.3 indicates the third core series from tree 4.

<i>Maximum period common to all cores (1807-1974)</i>							
1.1	1.2	2.1	2.2	3.1	4.1	4.2	4.3
1.1	- 0.47 <sup>a</sup>	-0.01	0.32	0.44	0.33	0.28	0.26
1.2	-	-0.10	0.50	0.43	0.27	0.21	0.28
2.1		-	0.46 <sup>a</sup>	0.23	0.63	0.67	0.61
2.2			-	0.57	0.68	0.64	0.68
3.1				-	0.41	0.33	0.39
4.1					-	0.96 <sup>a</sup>	0.96 <sup>a</sup>
4.2						-	0.96 <sup>a</sup>
4.3							-
$\bar{r}_{bt}$	= 0.39 (standard deviation = 0.21)						
$\bar{r}_{wt}$	= 0.76 (standard deviation = 0.27)						
$\bar{r}_{eff}$	= 0.43 from equation (3.43)						

<i>Maximum individual pair overlaps (years shown in parenthesis)</i>							
1.1	1.2	2.1	2.2	3.1	4.1	4.2	4.3
1.1	- 0.53(285) <sup>a</sup>	0.26(304)	0.48(294)	0.43(205)	0.26(304)	0.25(304)	0.10(304)
1.2	-	0.06(285)	0.46(285)	0.38(205)	0.28(285)	0.21(285)	0.15(285)
2.1		-	0.60(294) <sup>a</sup>	0.19(205)	0.29(325)	0.41(325)	0.21(325)
2.2			-	0.52(205)	0.41(294)	0.42(294)	0.28(294)
3.1				-	0.37(205)	0.26(205)	0.32(205)
4.1					-	0.92(445) <sup>a</sup>	0.92(463) <sup>a</sup>
4.2						-	0.89(445) <sup>a</sup>
4.3							-
$\bar{r}_{bt}$	= 0.30 (standard deviation = 0.12)						
$\bar{r}_{wt}$	= 0.77 (standard deviation = 0.19)						
$\bar{r}_{eff}$	= 0.33 from equation (3.43)						

<sup>a</sup>Indicates correlations among core series from the same tree.

quite accurate values provided a reasonable number of series and a reasonable span of annual values are used to calculate them. Empirical experiments, based on single-core-per-tree data, suggest that at least five series and a minimum of 30 years should be used (Briffa, 1984). Obviously, the more cores and, more importantly, the longer the period of analysis, the more representative the estimates will be of the population parameters. However, one important characteristic of tree-ring time series (indexed or not) is that the statistical quantities defined above are not constant in time. Indeed, they frequently vary markedly on decadal and century time scales.

Given a chronology with an equal number of cores per tree and uniform replication throughout its length, there will be little difference in results achieved using either the ANOVA method or a correlation matrix. However, if core depth is variable and the number of cores varies per tree, or if the time span varies greatly between individual cores, the method of estimating the signal parameters based on the matrix of maximum individual pair overlaps will be easier to apply.

As it is based on almost all, if not all, the data, it will go further toward overcoming the temporal instability in parameter estimation inherent in analyses based on restricted numbers of cores or years.

### 3.6.3. Estimating the chronology confidence

#### *Expressed Population Signal, Signal-to-Noise Ratio, and Subsample Signal Strength*

After estimating the strength of the statistical signals and their related noise parameters for a number of tree-ring series, it is necessary to quantify the degree to which the chronology signal is expressed when series are averaged.

Uncommon variance (noise) will cancel in direct proportion to the number of series averaged. In a simple example where a chronology comprises  $t$  trees with only a single core per tree, the variance of each series of indices is made up of the common signal,  $\bar{r}_{bt}$  (in this case also equivalent to  $\bar{r}_{\text{eff}}$ , and  $V(Y)$  in ANOVA), and noise,  $1 - \bar{r}_{bt}$ . Averaging reduces the noise to  $(1 - \bar{r}_{bt})/t$  while the common variance is unaffected. Therefore, the mean chronology has a total variance (signal + residual noise) of  $\bar{r}_{bt} + (1 - \bar{r}_{bt})/t$ . The chronology signal, expressed as a fraction of the total chronology variance, then quantifies the degree to which this particular sample chronology portrays the hypothetically perfect chronology. This has been termed the Expressed Population Signal or EPS (Briffa, 1984; Wigley *et al.*, 1984):

$$\text{EPS}(t) = \frac{\bar{r}_{bt}}{\bar{r}_{bt} + (1 - \bar{r}_{bt})/t} = \frac{t \bar{r}_{bt}}{t \bar{r}_{bt} + (1 - \bar{r}_{bt})} , \quad (3.44)$$

where  $t$  is the number of tree series averaged – one core per tree – and  $\bar{r}_{bt}$  is the mean between-tree correlation.

A more general expression for EPS, where a chronology has more than one core per tree, can be obtained by replacing  $\bar{r}_{bt}$  with  $\bar{r}_{\text{eff}}$  in equation (3.44) and using the number of trees sampled as  $t$ .

In a sample group of trees such as that used to produce *Table 3.4* where in any one year four trees with 2, 2, 1, and 3 cores, respectively, might be averaged,  $c_{\text{eff}}$  would be 1.7. Using the lower matrix estimates from *Table 3.4* of 0.30 and 0.77 for  $\bar{r}_{bt}$  and  $\bar{r}_{wt}$ , respectively, equation (3.40) gives  $\bar{r}_{\text{eff}} = 0.33$  and, hence, an EPS value, based on  $t = 4$  trees, of 0.66.

EPS is formally equivalent to the  $R_N^2$  (the expected correlation between the  $t$ -series average and the hypothetical population average) derived from first principles by Wigley *et al.* (1984) for the case of one core per tree. In this instance, it is also equivalent to the *percent common signal* defined by Cropper (1982) as

$$\text{PERCENT COMMON SIGNAL} = \frac{\text{SNR}}{1 + \text{SNR}} , \quad (3.45a)$$

where

$$\text{SNR} = \frac{t V(Y)}{1 - V(Y)} , \quad (3.45b)$$

where  $t$  is the number of series, and  $V(Y)$  defined in *Table 3.3* is used as the measure of the chronology signal. Because it uses  $\bar{r}_{bt}$  as the chronology signal, the percent common signal is not the same as EPS in which there is more than one core per tree.

SNR values (invariably the maximum value for a chronology, i.e., the value relating to the section of the chronology composed of the maximum number of cores) are often quoted as a measure of chronology quality (e.g., De Witt and Ames, 1978). This is clearly a difficult quantity to interpret because it has no upper bounds and its use for comparing chronologies is problematical. SNR behaves in a markedly nonlinear fashion – as a function of the number of trees. For large SNR, large increases in SNR lead to only minimal changes in EPS. The latter is easier to interpret.

However, EPS (or SNR) is not often a constant over the different parts of a chronology. It is important to appreciate the degree to which EPS varies through time as a function of variations in  $r$  and series replication. [It is not generally realized how variable all  $r$  values can be. However, the most important source of EPS variations is series replication, as equation (3.44) is relatively insensitive to variations in  $\bar{r}_{\text{eff}}$ .] *Figure 3.14* illustrates how EPS varies as a function of tree replication for a range of underlying  $\bar{r}_{\text{eff}}$  signals. The horizontal axis shows the number of trees in the chronology and three EPS curves are shown, each representing a different  $\bar{r}_{\text{eff}}$  value, equation (3.43). EPS rises asymptotically toward 1.0 as the number of trees tends to infinity. It rises very quickly as the number of trees increases from 1 to around 10 (for all values of  $\bar{r}_{\text{eff}}$ ), but progressively slowing for more than 10.

When  $\bar{r}_{\text{eff}}$  or tree numbers are already fairly high, EPS can still be improved through  $\bar{r}_{\text{eff}}$ , which can be increased by changing the type or level of standardization. This, however, produces only a slight improvement in EPS. The increase is more rapid with increasing  $\bar{r}_{\text{eff}}$  when tree numbers are low (as might be the case in early years of a chronology), so here it is clearly helpful to use an optimal standardization method.

*Figure 3.14* clearly shows that the law of diminishing returns is relevant when considering what range of EPS values constitute acceptable statistical quality. A value of 0.85 is one reasonable choice suggested by Wigley *et al.* (1984). Chronologies with  $\bar{r}_{\text{eff}}$  values of around 0.6 [ $\bar{r}_{bt}$  values of around 0.6 are typical for arid-site conifers in the western United States, e.g., De Witt and Ames (1978)] require as few as four trees to achieve this value. At the other end of the range, chronologies with  $\bar{r}_{\text{eff}}$  values of 0.2 (at the lower end of the range found in deciduous sites in the UK), approximately 25 trees are required to reach an EPS of 0.85.

No specific value of EPS can be thought of as adequate or minimum to ensure that a chronology is suitable for climate reconstruction. The common

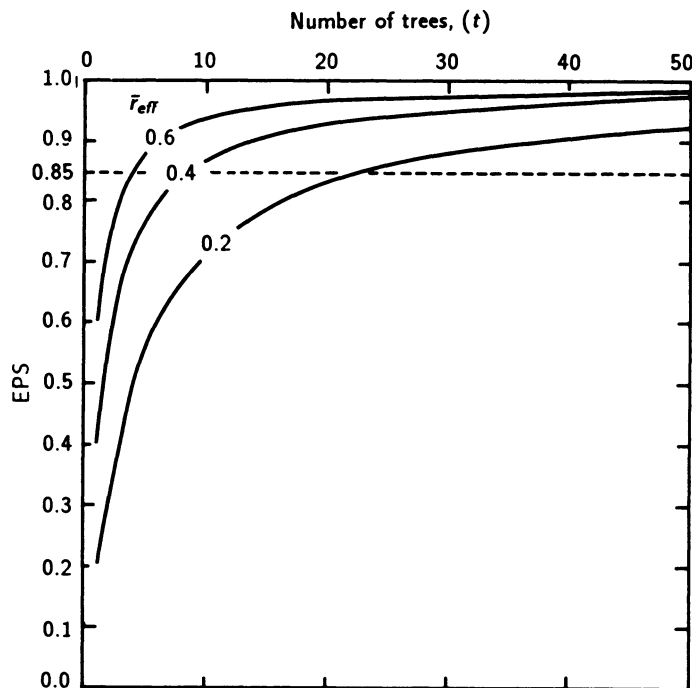


**Figure 3.14.** EPS values plotted as a function of the number of trees in a chronology for several example  $\bar{r}_{\text{eff}}$  values.

signal does not necessarily reflect only climate forcing (i.e., other common factors could include management, pests, pollution). Nonetheless, the use of some critical threshold can provide an objective, statistical benchmark for inter-chronology comparisons and for making quantitative judgments on the likely confidence of regression-based estimates made using chronologies with or without variable replication. One way of doing this is to select a value of EPS that is considered high enough to represent an acceptable level of chronology confidence and then quote the range of years for which EPS values equal or exceed this.

#### *Relationships Between the EPS and the Chronology Standard Error*

Fritts (1976, page 290) discusses the way in which chronology error can be gauged using the standard error (SE) calculated from the component variances of an ANOVA analysis (c.f. Table 3.9). He defined the SE as

$$\text{SE}^2 = \frac{V(YT)}{t} + \frac{V(YCT)}{et} , \quad (3.46)$$

where the  $V(YT)$  is the variance component due to differences in trees, the  $V(YCT)$  is the component due to differences in individual core chronologies (i.e., the between-tree and within-tree noise components), and  $t$  and  $c$  are the numbers of trees and cores per tree, respectively [note, equation (3.46) assumes  $V(YC) = 0$ ]. SE can easily be written in terms of  $\bar{r}_{\text{eff}}$  as shown below.

Fritts calculated SE values for different numbers of trees and different numbers of cores per tree for a small sample of *Pinus longaeva* indices to illustrate that on purely statistical grounds, given the same overall number of cores, the chronology with least error is always achieved by taking one core per tree rather than by sampling trees more than once. There are, however, as he points out, sometimes good practical reasons for adopting the latter strategy.

Fritts' SE values (1976, page 291) were calculated using absolute variance components, rather than the more easily compared values based on fractional variances (which can be calculated by dividing Fritts' SE values by the square root of the total variance component). If the fractional variance components are used, the equivalence between the EPS and the SE (for normalized core indices) can be shown to be

$$\text{SE}^2 = \frac{1 - \text{EPS}}{t(1 - \text{EPS}) + \text{EPS}} \quad (3.47)$$

in terms of the number of trees,  $t$ . From this, an EPS of 0.85 is equivalent to an  $\text{SE}^2$  of  $1/(t + 5.67)$ . Alternatively, SE can be expressed as

$$\text{SE}^2 = \frac{\bar{r}_{\text{eff}}(1 - \text{EPS})}{\text{EPS}} \quad . \quad (3.48)$$

An EPS of 0.85 is therefore equivalent to an SE of 0.325 for a relatively high  $\bar{r}_{\text{eff}}$  value of 0.6, but is equivalent to an SE of 0.188 when  $\bar{r}_{\text{eff}}$  is only 0.2. By replacing EPS in equation (3.48) with equation (3.44) using  $\bar{r}_{\text{eff}}$ , the SE can be expressed as

$$\text{SE}^2 = \frac{1 - \bar{r}_{\text{eff}}}{t} \quad (3.49)$$

in terms of the chronology signal,  $\bar{r}_{\text{eff}}$ , and the number of trees,  $t$ . *Figure 3.15* illustrates equation (3.49) plotted for a range of  $\bar{r}_{\text{eff}}$  values.

### *The Subsample Signal Strength (SSS)*

The EPS is an absolute measure of chronology error that determines how well a chronology based on a finite number of trees approximates the theoretical population chronology from which it is assumed to have been drawn. It may not, however, always represent the most relevant estimate of chronology confidence

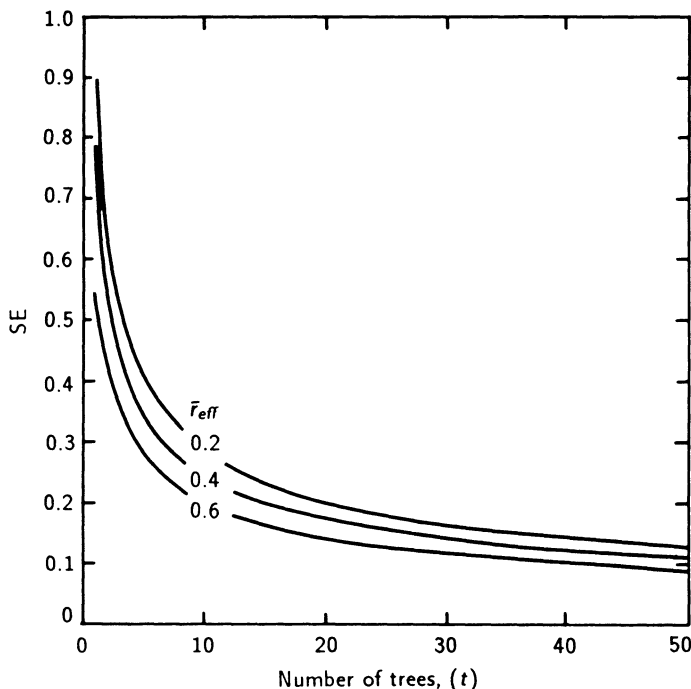


**Figure 3.15.** The standard error of a chronology plotted as a function of the number of constituent trees for several  $\bar{r}_{\text{eff}}$  values.

as a function of decreasing tree number. In dendroclimatology, a statistical link between climate and one or more chronologies is usually established by regression analysis. Frequently, this link is calibrated against a recent section of chronology data often made up of the maximum number of individual tree series ( $t$ ). Reconstruction estimates can then be made using earlier sections of chronology data. These tend to be made up of few tree series ( $t'$ ), generally even fewer as one goes further back in time. As  $t'$  becomes smaller there must be an absolute increase in chronology error (measured by the falling EPS) and hence an additional reduction of reconstruction confidence beyond that quantified in the calibration equation.

To measure this additional uncertainty, we can pose a general question: How representative is a  $t'$ -tree chronology of a  $t$ -tree chronology where  $t'$  is less than  $t$ ? The question may be answered by quantifying how well a chronology based on a subset of  $t'$ -tree series estimates a larger  $t$ -series chronology.

Wigley *et al.* (1984) derived an equation that describes the variance in common between a  $t'$ -core subsample and the  $t$ -core chronology, assuming that there is only one core per tree. They define a quantity, the subsample signal strength (SSS), as

$$SSS = \frac{t'[1 + (t - 1)\bar{r}]}{t[1 + (t' - 1)\bar{r}]} . \quad (3.50)$$

The  $t$  and  $t'$  are the number of cores in the sample and subsample, respectively. In the case where only one core per tree was involved, the  $\bar{r}$  is the  $\bar{r}_{bt}$  described earlier, equation (3.39a). Equation (3.50) has been validated empirically by comparing the theoretical estimates with those obtained by averaging individual values of subsample chronology correlations over large numbers of randomly chosen subsets (Briffa, 1984; Wigley *et al.*, 1984). Where multiple cores are available,  $\bar{r}_{\text{eff}}$  should be used, and  $t'$  and  $t$  become the number of trees in the subsample and reference chronologies, respectively.

The SSS can also be calculated as

$$SSS = \frac{\text{EPS}(t')}{\text{EPS}(t)} . \quad (3.51)$$

In calculating SSS using equation (3.51), the EPS values should be defined using equation (3.44) with  $\bar{r}_{bt}$  replaced by  $\bar{r}_{\text{eff}}$  (note that  $\bar{r}_{bt} = \bar{r}_{\text{eff}}$  when there is only one core per tree).

#### *Defining Acceptable Chronology Confidence Based on the SSS*

As with the EPS, just what constitutes an acceptable SSS level must ultimately be a subjective choice, and different criteria may be applied in different applications. Wigley *et al.* (1984) suggest that in climate reconstruction work, SSS values should be sufficiently large to ensure that any reconstruction uncertainty arising from decreasing core numbers should be *considerably less* than that quantified in the calibration of the chronology-climate link. In effect, this would require a critical or threshold SSS value for defining acceptable chronology uncertainty, substantially above that of the amount of climate variance explained by the fitted equation(s).

As an illustration, they show that for a climate reconstruction with 50% explained variance an SSS threshold of 0.85 (equivalent to allowing a maximum additional reconstruction uncertainty of 15%) would reduce the explained climate variance to around 43% ( $50\% \times 0.85$ ). Their choice of an SSS of 0.85 was given only as an illustration. A general acceptance of this figure would ensure that additional chronology error was always restricted to a maximum of 15%.

It would not always be desirable or practicable to withhold potentially useful chronologies in climatic reconstruction solely on the basis of poor chronology confidence. Chronologies, or sections of chronologies, with only moderately high EPS or SSS values might still be highly correlated with climate parameters. It is important, however, to be aware of the true extent of uncertainty that is inherent in the estimates of past climate based on such chronologies. In any particular reconstruction case, the magnitude of regression coefficients define which specific chronologies are most important to the reconstructions. Provided these

specific chronologies are of good statistical quality, then lower EPS or SSS values could be accepted for others.

Alternatively, one could use a single SSS cutoff for defining usable portions of chronologies such as the figure of 0.85 used to construct *Figure 3.16*. This shows, for a  $t$ -tree chronology with a particular  $\bar{r}_{\text{eff}}$  signal, the minimum number of trees required for a  $t'$ -tree subset to maintain an SSS above 0.85. Reconstructions based on these portions of chronologies are subject to additional reconstruction uncertainty (over that of the calibration estimates) of no more than 15%. The points on *Figure 3.16* illustrate the minimum number of trees required to maintain an SSS above 0.85 in the same chronologies used in the following comparison of standardization methods.

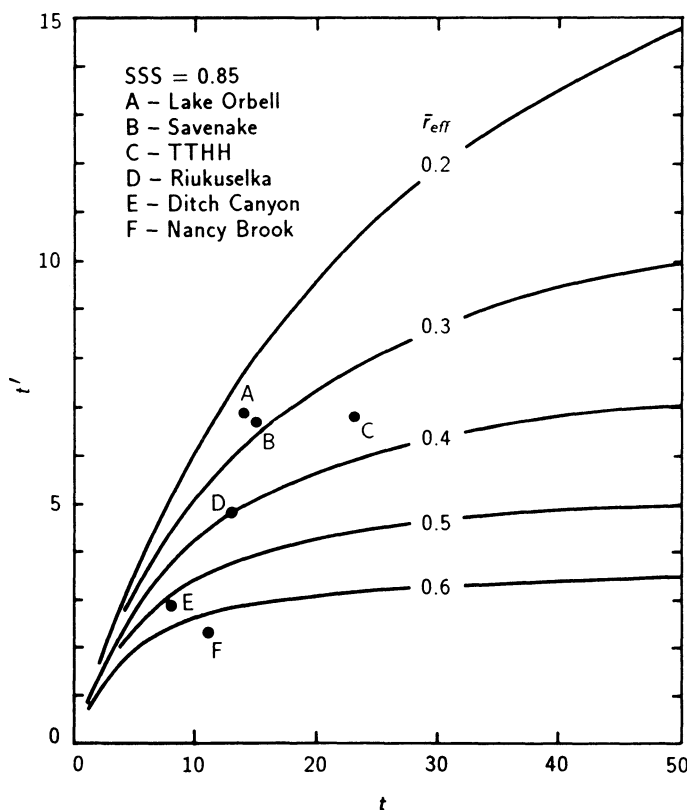


**Figure 3.16.** The number of trees ( $t'$ ) necessary in a subsample chronology to maintain the SSS above 0.85 where the reference chronology is composed of  $t$  trees. Curves are shown for several different  $\bar{r}_{\text{eff}}$  values. The values for a number of chronologies are shown as examples. These are the same chronologies used in the comparison of standardization methods in Section 3.7. The minimum number of trees required to reach SSS equal to 0.85 varies from three to seven.

### 3.7. A Comparison of Some Tree-Ring Standardization Methods

*E. Cook and K. Briffa*

This chapter has described a large array of techniques that can be used for standardizing ring widths and creating a mean chronology of tree-ring indices. In this section, some of the methods will be applied to six different collections of ring-width data. The results will be compared with the known characteristics and history of each tree-ring site and the known statistical properties of the ring-width data. These comparisons will highlight the strengths and weaknesses of the methods of the known properties of the data being standardized. However, they are not intended to determine if one method is superior to the others. While some techniques may work well in many situations, there is probably no one method that is universally superior.

The strengths and weaknesses of any tree-ring standardization method will be largely determined by the properties of the data being standardized and by the intended use of the standardized data. The definition of the expected signal (Briffa *et al.*, 1987) in the tree-ring data must be considered prior to selecting the method of standardization. Only after the signal has been defined can an appropriate method of standardization be chosen to minimize the noise. Thus, the definition of noise will be determined by the prior definition of the signal. Once a method is chosen, the ring-width data can be standardized to produce an estimate of the expected signal, which we will call the observed signal (Briffa *et al.*, 1987). Unlike most statistical estimators of population parameters, no statistical theory tells us how well the observed signal in tree rings estimates the expected signal. In most cases, we must rely on statistical measures of signal strength, frequency domain definitions of signal and noise, and knowledge about sites, stand histories, and tree biology to guide us.

#### 3.7.1. Ring-width data sets

The six data sets used in this study were selected to provide a range of stochastic properties and standardization problems. The data sets reflect differences owing to species biology, site character, and disturbance or management history. A brief description of each ring-width data set will be given next.

##### *Ditch Canyon (DC)*

The species is ponderosa pine (*Pinus ponderosa*). The site is in the low-elevation, discontinuous coniferous forest zone of the southwestern United States, which has produced some of the finest tree-ring chronologies for dendroclimatic studies. The sampled trees are in an open-canopy stand, with minimal competition among trees and no known disturbance history. A chronology developed from these ring-width series has excellent statistical properties for dendroclimatic studies (Fritts and Shatz, 1975). The growth trends of the ring-width series are largely negative exponential in form. High-frequency variations (time scale < 10

years) in ring width are large and only moderately autocorrelated. This collection has the fewest potential standardization problems of the six data sets and comes closest to a control for comparing the different methods.

#### *Twisted Tree-Heartrot Hill (TTHH)*

The species is white spruce (*Picea glauca*). The site is in the discontinuous forest-tundra ecotone region of the Yukon Territory, Canada, and has been described previously in Jacoby and Cook (1981). The sampled trees are in an open-canopy stand with low competition among trees and no known history of disturbance. The growth trends tend to be negative exponential or linear in form, with a high proportion of the latter trends being positive in slope. The yearly variations in ring width are relatively small and dominated by very strong low-frequency fluctuations (time scale > 50 years) that are usually common to all trees. As a consequence, the ring-width series are highly autocorrelated even after any apparent trend has been removed. Although this collection has few standardization problems, the very strong low-frequency fluctuations and high autocorrelation make the series more sensitive to the method of detrending and any manipulation of the persistence structure.

#### *Riukuselka (RIUK)*

The species is Scots pine (*Pinus sylvestris*). The site represents old, unmanaged coniferous forest, typical of northern Scandinavia. The sampled trees were in relatively open habitat at the top of a hill less than 100 meters below the natural timberline. The sampled trees range in age from about 250 to over 450 years, with the majority in the range of 250–350 years. Competition among trees is not a significant factor affecting the age trends of the individual ring-width series. Consequently, the ring widths show a classic deterministic-type age-related decline over the length of each series. However, other than this, the series show relatively little variance at low frequencies (time scales > 50 years). Medium-frequency fluctuations (time scales > 10 and < 50 years) appear to be synchronous among most series.

#### *Nancy Brook (NB)*

The species is red spruce (*Picea rubens*). The site is in a montane boreal forest, typical of the higher elevations of the northern Appalachian Mountains in eastern North America. The ring-width series range from about 200 to 370 years in age, with the majority in the range of 250–300 years. The sampled trees were growing in a closed-canopy, old-growth stand with no known cutting history. Competition for light among neighboring trees is great, and the structure of the stand is strongly affected by gap-phase stand dynamics. This is reflected in the medium-frequency fluctuations (10–50 year) of ring width, which are frequently out-of-phase between trees owing to competition and disturbances. These and the longer-term growth trends are highly stochastic in form and variable among trees. The yearly variations in ring width are dominated by these low- and

medium-frequency fluctuations. This collection is an excellent example of tree-ring data having a common signal that is strongly contaminated by competition effects in the stand. It is a more difficult standardization problem compared with the previous three cases.

### *Lake Orbell (OBL)*

The species is silver beech (*Nothofagus menziesii*), a Southern Hemisphere evergreen beech. The collection of 20 ring-width series is from a site near the alpine timberline on the southern island of New Zealand. The ring-width series exceed 200 years of age. The site and stand have been described previously by Norton (1983a). It is a closed-canopy forest of mixed *Nothofagus* species where competition among trees is likely to be high. Consequently, the long-term growth trends tend to be disturbed by competition in the stand.

### *Savenake (SA V)*

The species is the European pedunculate oak (*Quercus robur*). The site is typical of an *ancient* English parkland wood. It forms part of a royal forest, which has been managed for centuries, and is commercially managed today. The sampled trees were typically between 200–300 years of age. The sampled trees are growing in relatively open forest, but the density of trees is great enough to mean that competition will be a significant factor influencing the evolution of the *biological* or age-related growth curves of the individual trees. Sampling was restricted to an area of forest of about one hectare.

#### **3.7.2. Methods of standardization and statistical assessment**

Four methods of standardization were performed on each data set: linear and negative exponential detrending (LE), spline detrending using the 67% $n$  criterion (SP), 67% $n$  spline detrending and autoregressive modeling (AR), and filtering with a 60-year Gaussian low-pass filter (GF). Each method has been described earlier. The LE and GF methods represent the extremes in terms of growth-curve flexibility, with the former being the most rigid and the latter the most flexible. Thus, in terms of trend removal and its ultimate effect on low-frequency variance, the LE and GF methods should provide the sharpest contrasts, with the SP and AR methods falling somewhere in between. The SP and AR methods only differ in terms of autoregressive modeling, which may have more subtle effects on the final chronology.

The summary statistics used for comparing each standardization method are mean sensitivity (MS), standard deviation (SD), coefficient of skew (SK), coefficient of kurtosis (KT), lag-1 autocorrelation coefficient (R1), and the average correlation among trees for the common overlap period among series [RBar; equation (3.39a)]. The MS, SD, and R1 statistics are frequently used to assess the statistical-dendroclimatological quality of tree-ring chronologies (Fritts and Shatz, 1975; Fritts, 1976). The SK and KT statistics are included to assess any

higher-order effects on the probability distribution owing to the method of standardization. The time period used for all but the RBar comparisons was 1701–1975 for each data set – except Ditch Canyon, which was 1701–1971. No RBar values are included for the AR chronologies because this method uses prewhitened indices rather than simple detrended indices, which contain autocorrelation. Hence, the AR RBar may not be strictly comparable with that computed using the other standardization methods. In addition, the RBar for site SAV is a weighted average of the inter-series correlations over the maximum possible overlap period between series because the ring-width series do not overlap sufficiently.

Besides these summary statistics, we will look at the correlations among the chronologies developed by the different standardization methods and use spectral analysis to search for frequency-dependent effects. Each spectrum is computed from 55 lags of the autocorrelation function and smoothed with the Hamming window.

*Table 3.5* shows the summary statistics for the six sites and four standardization methods. It is readily apparent that most of the statistics are extremely similar regardless of the method of standardization. The greatest differences are seen in R1 and RBar. Differences in R1 reflect how much low-frequency variance has been removed by each method. The LE method generally removes the least; the GF method, defined by the 50% cutoff of 60 years, removes the most. However, the way in which this low-frequency variance removal translates into the estimates of RBar is not predictable. In some cases (i.e., site DC and NB), the RBar increases from LE to GF; in other cases (i.e., TTHH and SAV), the RBar decreases from LE to GF. The differences in performance reflect the differences in the low-frequency properties of the raw data. For both DC and especially NB, most of the out-of-phase variance between series is in the wavelengths longer than about 60 years in duration. A 60-year low-pass filter performs better in removing this variance than does a negative exponential or linear regression curve, hence the increased RBar using the GF method. In contrast, both the TTHH and SAV ring-width collections have lower-frequency fluctuations that tend to be in phase. A 60-year low-pass filter removes most of this in-phase variance, which leads in these cases to a reduced RBar.

The correlations between chronologies as a function of the standardization method are shown in *Table 3.6*. The correlations are usually high and often greater than 0.95. However, some are quite low, i.e., 0.68 (LE versus GF) for site TTHH. The greatest differences are found between the LE, SP, and GF methods, with AR being very similar to SP. These differences largely reflect how much low-frequency variance has been left in the final chronology by each standardization method. This fact is graphically revealed in the variance spectra of the different chronologies [*Figures 3.17(a-f)*]. Virtually all of the significant ( $\alpha = .20$ ) differences between chronologies are in the low frequencies, with the 60-year GF method being most different by far. This is not surprising considering that most of the variance in the original ring widths is composed of low-frequency growth trends and fluctuations. At wavelengths shorter than about 20 years in duration, more subtle differences are apparent. However, it is impossible to say to what extent they are meaningful with regard to the intended application.

**Table 3.5.** Within-series summary statistics for the tree-ring standardization tests: mean sensitivity (MS); standard deviation (SD); lag-1 autocorrelation (R1); coefficient of skew (SK); coefficient of kurtosis (KT); average correlation between trees for the common overlap period among series (RBar); linear-exponential detrending (LE); 67% spline detrending (SP); autoregressive modeling (AR); 60-year Gaussian low-pass filter (GF).

<i>Site: Ditch Canyon (DC)</i>		<i>Standardization method</i>			
<i>Statistics</i>		<i>LE</i>	<i>SP</i>	<i>AR</i>	<i>GF</i>
MS		.382	.385	.387	.392
SD		.391	.374	.374	.367
R1		.416	.383	.367	.256
SK		.092	.009	-.028	-.038
KT		2.905	2.774	2.858	2.869
RBar		.598	.609	—	.721
<i>Site: Twisted Tree-Heartrot Hill (TTHH)</i>					
MS		.126	.125	.126	.125
SD		.224	.186	.185	.126
R1		.773	.655	.627	.223
SK		.079	-.074	-.077	.198
KT		2.394	2.879	2.866	3.215
RBar		.380	.399	—	.345
<i>Site: Riukuselka (RIUK)</i>					
MS		.169	.169	.176	.171
SD		.262	.250	.251	.201
R1		.692	.669	.635	.402
SK		-.026	-.014	-.096	-.019
KT		2.871	2.780	2.791	3.235
RBar		.454	.521	—	.526
<i>Site: Nancy Brook (NB)</i>					
MS		.114	.116	.118	.116
SD		.182	.142	.142	.133
R1		.708	.515	.465	.399
SK		.224	.017	.087	.053
KT		3.178	3.613	3.866	3.826
RBar		.218	.383	—	.363
<i>Site: Lake Orbell (LO)</i>					
MS		.263	.264	.272	.264
SD		.314	.295	.278	.260
R1		.398	.337	.211	.166
SK		.628	.457	.431	.222
KT		3.843	3.598	3.595	3.092
RBar		.270	.370	—	.316
<i>Site: Savenake (SAV)</i>					
MS		.148	.148	.161	.147
SD		.189	.178	.193	.166
R1		.506	.465	.474	.388
SK		.372	.201	.052	.017
KT		2.931	2.763	2.625	2.795
RBar		.397	.327	—	.344

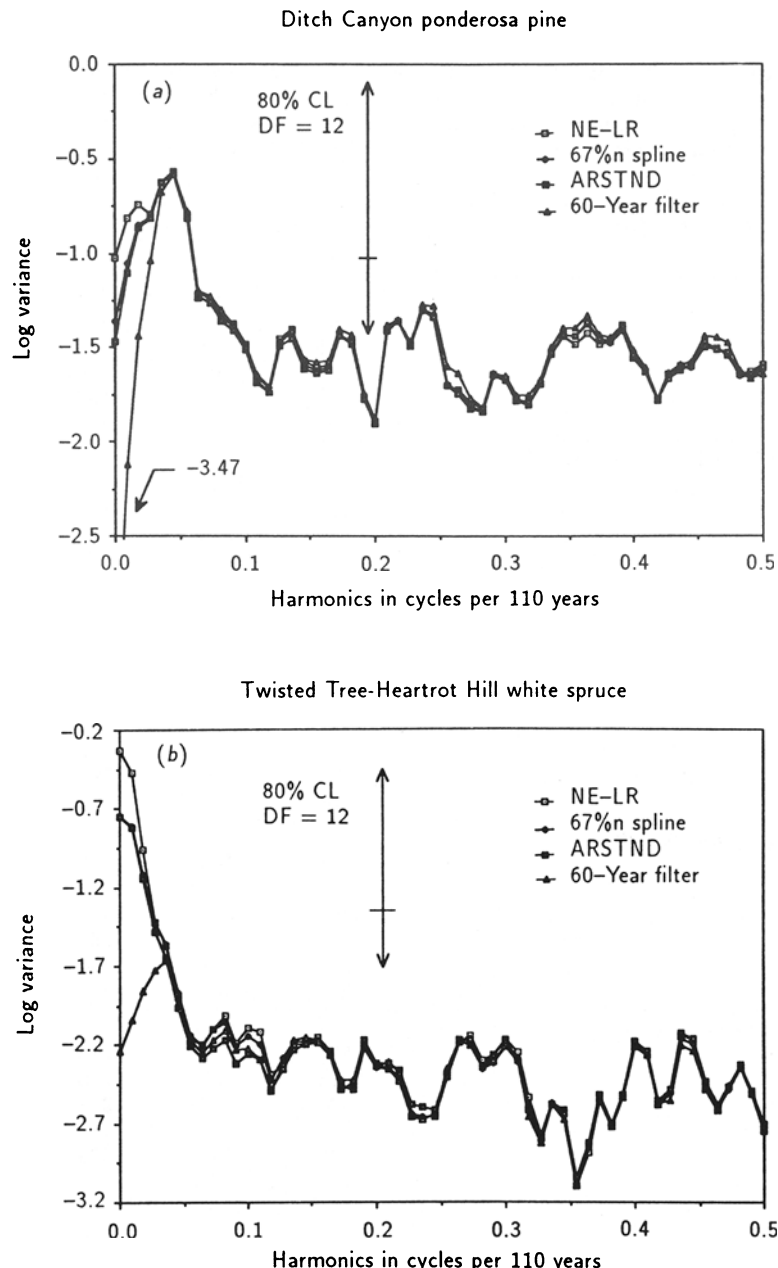


**Figure 9.17.** The variance spectra of the tree-ring chronologies for six sites produced by four different methods of standardization: (a) Ditch Canyon; (b) Twisted Tree-Heartrot Hill; (c) Nancy Brook; (d) Riukuselka; (e) Lake Orbell; (f) Savenake. Each spectrum is computed from 55 lags of the autocorrelation function and smoothed with the Hamming window.

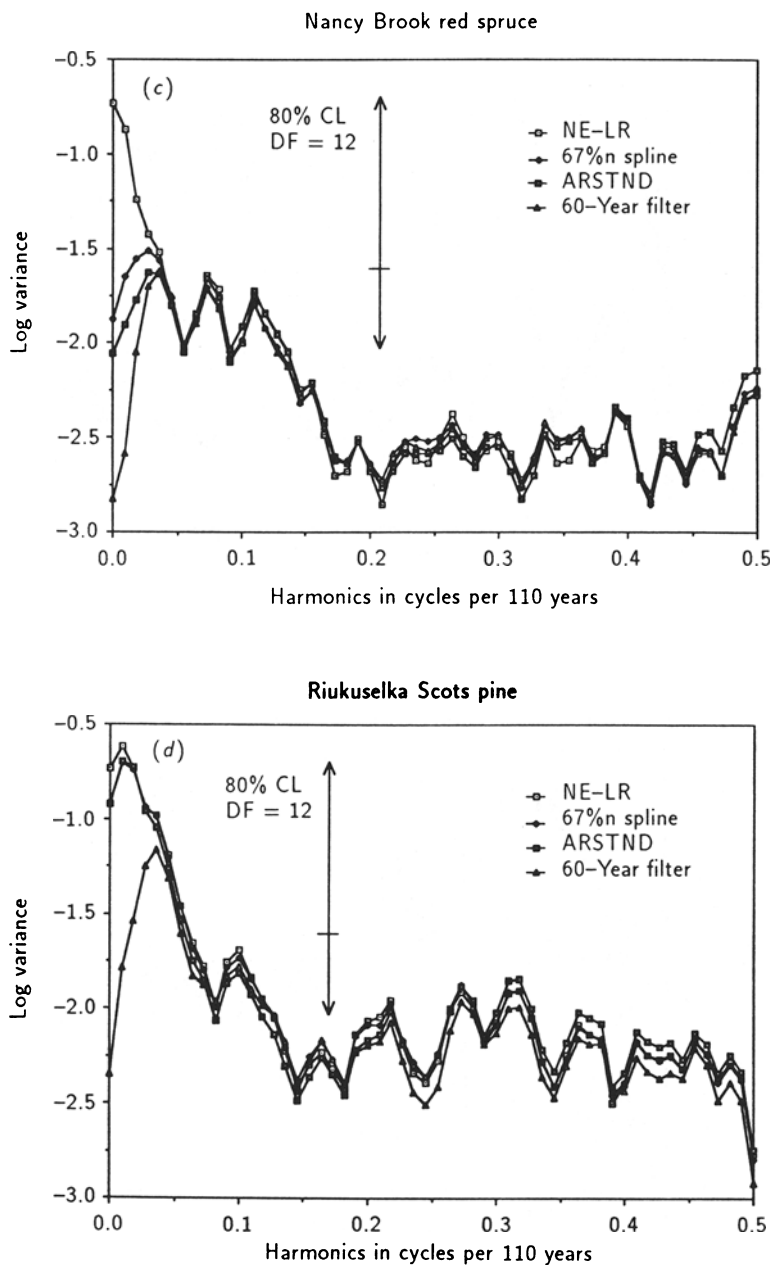
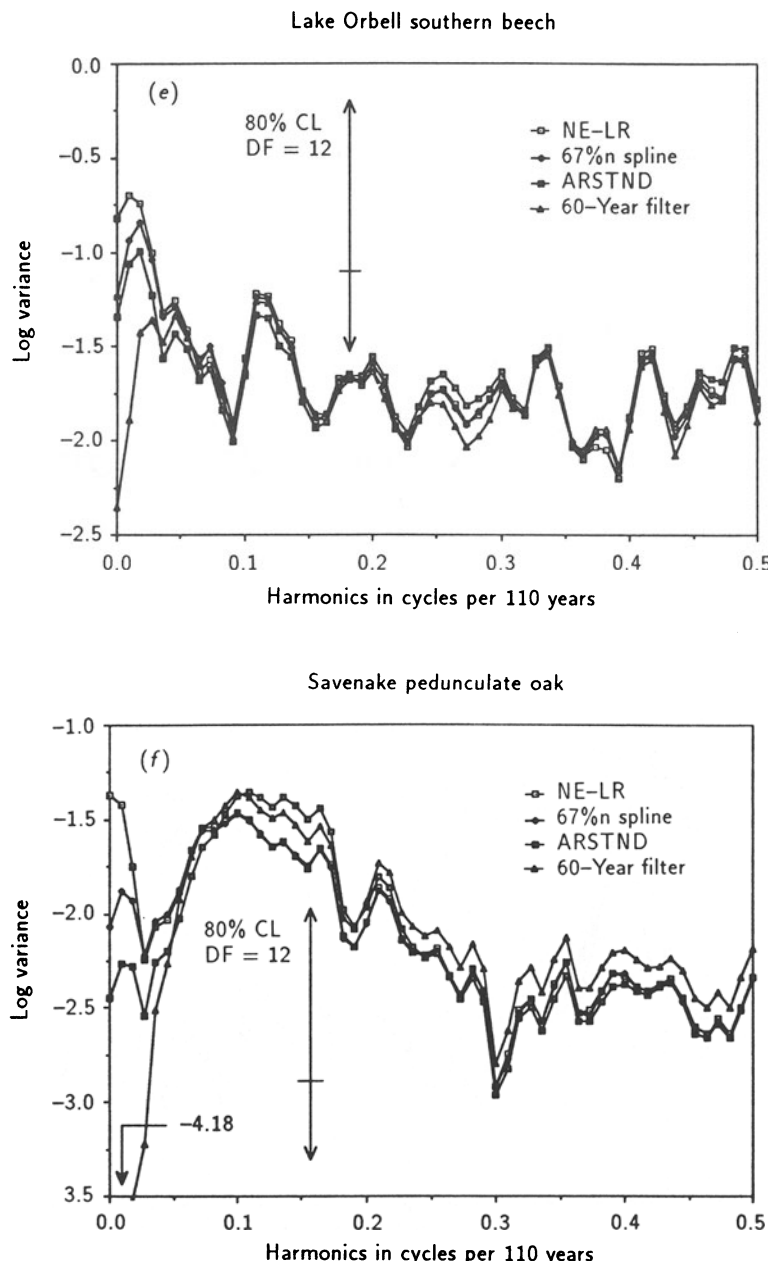


Figure 8.17. Continued.



**Figure 8.17.** Continued.

**Table 3.6.** Correlations between the chronologies of each site developed by the four standardization methods. The standardization methods are linear-exponential detrending (LE); 67%  $n$  spline detrending (SP); autoregressive modeling (AR); 60-year Gaussian low-pass filter (GF).

<i>Ditch Canyon</i>				<i>TTHH</i>				
	LE	SP	AR	GF	LE	SP	AR	GF
LE	1.00	0.99	0.98	0.94	1.00	0.95	0.94	0.68
SP		1.00	1.00	0.97		1.00	0.99	0.82
AR			1.00	0.97			1.00	0.81
GF				1.00				1.00
<i>Ruikuselka</i>				<i>Nancy Brook</i>				
	LE	SP	AR	GF	LE	SP	AR	GF
LE	1.00	0.99	0.98	0.87	1.00	0.81	0.79	0.78
SP		1.00	0.99	0.90		1.00	0.98	0.96
AR			1.00	0.89			1.00	0.97
GF				1.00				1.00
<i>Lake Orbell</i>				<i>Savenake</i>				
	LE	SP	AR	GF	LE	SP	AR	GF
LE	1.00	0.98	0.97	0.91	1.00	0.98	0.93	0.93
SP		1.00	0.99	0.95		1.00	0.96	0.97
AR			1.00	0.95			1.00	0.92
GF				1.00				1.00

The very small differences between the SP and AR chronologies reflect the fact that autoregressive modeling has its strongest effect on the error variance of the mean-value function, a characteristic that we have not reported on here because of the AR method.

### 3.7.3. Conclusions

These comparisons indicate that the method of standardization can have profound effects on the resultant chronology. These effects are most readily seen in the variance spectrum where they are largely restricted to the lowest frequencies. Depending on the application of the tree-ring chronology and the definition of signal and noise, an *a priori* decision must be made about what will be retained as signal (or discarded as noise) in the low frequencies of tree-ring data. We do not propose any guidelines for making this decision because it is likely to be completely data and application dependent. However, we strongly caution the user of any tree-ring standardization method to think carefully about the definitions of signal and noise, as they pertain to the tree-ring application at hand, the site from where the tree-ring data came, and the frequency-domain properties of the raw tree-ring data. And, never use any tree-ring standardization method or computer program as a *black box*.

This chapter has covered a wide range of concepts and statistical techniques useful in developing tree-ring chronologies for environmental studies.

Tree-ring series will be used increasingly in the future as monitors of environmental change for the simple reason that they are available where no other comparable long-term environmental sensors exist. In the process, the statistical methods used to analyze tree rings will change and improve. Thus, we do not claim any timelessness in the methods we have described. However, we hope that the chapter will provide a reference for the present and a basis for future developments in the science.